AD-A089 850 JAYCOR DEL MAR CA F/G 17/2
USE OF ELECTRO-OPTIC TECHNIQUES TO ACHIEVE ELECTROMAGNETIC PULS--ETC(U)
JUN 80 R A GREENWELL, W A RADASKY N66001-79-C-0191

UNCLASSIFIED NOSC-TR-564 NL

NOSC

END
DATE
FILMED
11-80
DTIC

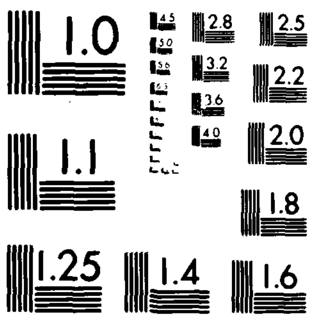

MICROCOPY RESOLUTION TEST CHART
NATIONAL BUREAU OF STANDARDS-1963-A

LEVEL II

12

NOSC

NOSC TR 564

NOSC TR 564

Technical Report 564

USE OF ELECTRO-OPTIC TECHNIQUES TO ACHIEVE ELECTROMAGNETIC PULSE HARDNESS

Determination of the effectiveness of optical fiber and hardwired interface technologies in military communication systems in a nuclear environment

RA Greenwell (NOSC)
JAYCOR, Del Mar, CA

(Contract N66001-79-C-0191)

12 June 1980

Final Report for period September 1979-April 1980

Prepared for
DEFENSE NUCLEAR AGENCY
RAEV
Alexandria, VA 20305

Approved for public release; distribution unlimited

NAVAL OCEAN SYSTEMS CENTER
SAN DIEGO, CALIFORNIA 92152

NAVAL OCEAN SYSTEMS CENTER, SAN DIEGO, CA 92152

AN ACTIVITY OF THE NAVAL MATERIAL COMMAND

SL GUILLE, CAPT, USN
Commander

HL BLOOD
Technical Director

ADMINISTRATIVE INFORMATION

Work was conducted under NOSC direction through contract N66001-79-C-0191 to Jaycor, Del Mar, CA, as part of the Guidelines for EMP Hardening Using Electro-Optic Techniques Program of the Defense Nuclear Agency (RAEV) under Program Element RDDA, work unit CG53. This report covers work from September 1979 to April 1980 and was approved for publication 12 June 1980.

The major Jaycor contributors to this study were WH Hardwick, WA Radasky, and TM Flanagan.

Released by
FM Tirpak, Head
Sensors Division

Under authority of
RE Shutters, Head
Surface/Aerospace
Surveillance Department

METRIC CONVERSION

To convert from	to	Multiply by
rad (rd)	gray (Gy)	10^{-2}
calorie per gram (cal/g)	joule per kilogram(J/kg)	4.184×10^3
ton (nuclear equivalent of TNT)	joule (J)	4.184×10^9

UNCLASSIFIED (19) TR-564

SECURITY CLASSIFICATION OF THIS PAGE (When Data Entered)

REPORT DOCUMENTATION PAGE		READ INSTRUCTIONS BEFORE COMPLETING FORM
1. REPORT NUMBER (18) NOSC Technical Report 564 (TR564)	2. GOVT ACCESSION NO. AD-A089850	3. RECIPIENT'S CATALOG NUMBER
4. TITLE (and Subtitle) (6) USE OF ELECTRO-OPTIC TECHNIQUES TO ACHIEVE ELECTROMAGNETIC PULSE HARDNESS. Determination of the effectiveness of optical fiber and hardwired interface technologies in military communication systems in a nuclear environment.		5. TYPE OF REPORT & PERIOD COVERED (9) Final rept. Sep[redacted]79 - Apr[redacted]80
		6. PERFORMING ORG. REPORT NUMBER
7. AUTHOR(s) (10) R.A. Greenwell [redacted] W.A. Kalinski ~~JAYCOR, Del Mar, CA (Contract N66001-79-C-0191)~~ W.H. Hardwick T.M. Flanagan		8. CONTRACT OR GRANT NUMBER(s) (15) N66001-79-C-0191
9. PERFORMING ORGANIZATION NAME AND ADDRESS Naval Ocean Systems Center San Diego, CA 92152		10. PROGRAM ELEMENT, PROJECT, TASK AREA & WORK UNIT NUMBERS RDDA, CG53
11. CONTROLLING OFFICE NAME AND ADDRESS Defense Nuclear Agency RAEV, Alexandria, VA 20305 (11)		12. REPORT DATE 12 Jun[redacted]80
		13. NUMBER OF PAGES 62
14. MONITORING AGENCY NAME & ADDRESS (if different from Controlling Office) (12) 65		15. SECURITY CLASS. (of this report) Unclassified
		15a. DECLASSIFICATION/DOWNGRADING SCHEDULE

16. DISTRIBUTION STATEMENT (of this Report)

Approved for public release; distribution unlimited.

17. DISTRIBUTION STATEMENT (of the abstract entered in Block 20, if different from Report)

18. SUPPLEMENTARY NOTES

19. KEY WORDS (Continue on reverse side if necessary and identify by block number)

Electro-optics
Fiber optics
Nuclear environment
Electromagnetic pulse (EMP)
Transient radiation effects (TRE)
Hardening

0.002

20. ABSTRACT (Continue on reverse side if necessary and identify by block number)

Fiber optics will reduce the susceptibility of systems to a direct EMP threat. Cables shorter than 10m present a tradeoff between the shielding effectiveness of standard cables and that of shielding around critical fiber optic receiver components. Long-haul ground systems require only electronics protection; the fiber optic cable is immune to em pickup and need not be buried for protection. Fiber optic susceptibility is less than that of hardwire to burnout and upset in systems that allow an outage time of 1 ms. In a steady-state or low-dose-rate environment, system vulnerability levels depend on fiber response and design margin. A fiber optic interface is feasible which will not fail under the dose rates and total dose levels equivalent to a natural space environment of 2×10^{-3} rad(Si) per second for 7 years.

DD FORM 1 JAN 73 1473 EDITION OF 1 NOV 65 IS OBSOLETE
S/N 0102-LF-014-6601

UNCLASSIFIED
SECURITY CLASSIFICATION OF THIS PAGE (When Data Entered)

392220

Fiber optic system electronics are no more vulnerable to total dose than those of hard-wired systems, which, at practical dose levels of 1Mrad, do not appear vulnerable. In fiber optic cables, vulnerability level depends on cable type and system design margin. Insufficient data exist to estimate vulnerability levels for fiber optic systems in displacement damage-producing environments.

The report contains a list of 70 references.

OBJECTIVE

Determine the effectiveness of optical fiber interface techniques when applied to other system interface technologies as a hardening measure against a nuclear environment. Evaluate the effects of electromagnetic pulse (EMP) and transient radiation (TRE) on electro-optic and other electronic devices and components within military communication systems.

RESULTS

Fiber optics will reduce the susceptibility of systems to a direct EMP threat. However, short cable lengths (less than ten metres) would present a tradeoff between the shielding effectiveness of standard cables and effectiveness of the shielding around critical components in the fiber optic receiver. For long-haul ground systems it is essential to protect only the electronics in the system since the fiber optic cable is immune to electromagnetic pick-up and need not be buried to protect it from the direct EMP threat.

For manned systems, where the associated transient radiation effects are related to personnel survivability, it is expected that a fiber optic system can easily meet the nuclear requirements. More shielding protection is necessary to eliminate any transient incapacitation of personnel than to protect the fiber optic interface. Tactical manned systems such as aircraft, mobile vans, ships, etc, are ideal candidates for fiber optic interfaces.

For systems that allow an outage time of 1 millisecond or more, caused by a prompt ionizing dose, fiber optics is less susceptible than hard-wired systems to burnout and upset. In a steady-state or low-dose-rate environment, vulnerability levels for the systems are highly dependent on the fiber response and the design margin. It is possible to design a fiber optic interface that will not have enough steady-state radiation-induced attenuation to fail when the dose rate and total dose levels are equivalent to a natural space environment, 2×10^{-3} rad(Si) per second for 7 years.

The electronics associated with fiber optic systems will be no more susceptible to the total dose than the electronics in a hard-wired system. However, at practical levels of total dose of one million rads(Si), no vulnerability of the cables has been detected in hard-wired systems. For fiber optic cables the vulnerability level is highly dependent on the type of cable and the system design margin. At the present time, insufficient data are available to estimate the vulnerability levels for fiber optic systems in displacement damage-producing environments.

RECOMMENDATIONS

1. Consider fiber optics in the design of any system whose cable runs are greater than 10 metres and which must adhere to military system EMP requirements.

2. Consider fiber optics in the design of any system whose recovery times are greater than 1 millisecond, and whose dose rate and total dose tolerance are within the link budget margin.

3. Consider fiber optics in the design of any system where personnel nuclear survivability requirements are the limiting factor.

4. Obtain additional data to ascertain the displacement damage-producing effects on fiber optic systems.

CONTENTS

INTRODUCTION

The Department of Defense requires an ever-increasing number of systems to be hardened to radiation specifications. Many variations in the specifications exist because of different operational system applications, nuclear weapon effects, and natural (space) environments. Among the nuclear weapons effects requirements, the hardening of a system to the electromagnetic pulse (EMP) environment for most systems is very costly and time-consuming. Therefore, the DoD has investigated, through many studies and programs, methods to reduce the cost and effort for accomplishing this task. One of the most promising methods, owing to its inherent immunity to electromagnetic effects, is the use of electro-optic techniques, primarily fiber optic coupled systems. However, these systems are vulnerable to other aspects of the nuclear environments. This report discusses the nuclear survivability tradeoffs involved when fiber optics are being considered as a hardening measure in the design of the system.

The approach taken is to calculate the radiation vulnerability levels of six classes of fiber optic systems for three different lengths of cables, thus considering a significant portion of military applications. The transient radiation effects (TRE) and EMP vulnerability levels of hard-wired technologies are compared within various radiation environments, and advantages and disadvantages of each technology are then identified. The final sections of the report present the data bases from which assumptions for the calculations were made, with suggestions for some of the radiation-hardening techniques that may be used for fiber optic systems.

Applications of fiber optic technology in systems that have EMP and radiation specifications are also discussed.

COMPARISON OF NUCLEAR VULNERABILITIES IN FIBER OPTIC AND HARD-WIRED SYSTEMS

To compare the nuclear vulnerabilities of fiber optic and hard-wired data links, it is first necessary to identify those critical operating parameters that will be affected by the nuclear environment. It is then necessary to model the radiation effects on those components that determine the critical parameters. Finally, susceptibility levels for the link's operating parameters must be established.

For fiber optic systems, this process can be very complex because of the interdependence of the operating parameters on all electro-optical components. Further, the response of most components to the radiation environment is not well known or characterized, and in some cases the basic radiation effects mechanisms have not been identified. To accomplish the comparison study, it is necessary that suppositions be made as to the response of the components. For this study, the suppositions have been based either on available data for the components or on basic radiation effects mechanisms that should be applicable, as discussed under Nuclear Vulnerabilities of Electro-Optic Components. In some instances, extrapolation of the data over several orders of magnitude has been made; this is always prone to error since the radiation response may be different at widely varying radiation levels.

In the case of the hard-wired systems, more data are available on the radiation effects on the possible component technologies that may be employed in implementation of the system, a summary of which is presented in the Radiation Effects on Electronic Systems section. However, for the critical area of the response of cables to nuclear environments,

much controversy exists in the radiation effects community as to the best methods of predicting radiation response. Furthermore, cable response is highly dependent on the particular geometry of the system. For this reason, highly complex computer codes have been developed to predict cable response, none of which performs the calculations needed to work the problem in reverse order, that is, given a component vulnerability level, calculate the radiation environment which will produce that vulnerability level in the component. In this section, the coefficients for the calculation of coupling to the cables have been taken from reference 1. A range of 40 to 80 dB has been estimated for the shielding effectiveness of cables used in the systems, which should include most of the cables considered for military applications. These calculations are not intended to precisely predict the magnitude of the radiation environment, but rather to establish a lower limit of the radiation environment at which vulnerability may occur. These are linear models, and the predictions at the higher levels where nonlinear effects may occur, although possibly inaccurate, have been included to show the trends.

The following tables present calculations for various radiation environments that will cause degradation of link performance to below specified values, complete failure of the links, or upsets in the electronics. Each table is accompanied by a discussion of the estimates that have been made in the radiation response of the components. The tables present radiation component values for six hypothetical systems, four digital and two analog, for three transmission path lengths. These systems and distances were selected because they cover a wide spectrum of the applications needed by military communications systems.

FIBER OPTIC DATA LINK RESPONSES TO RADIATION ENVIRONMENTS

The basic electro-optic system performance parameters are presented in table 1. The signal requirements are taken from the minimum signal power required to establish a signal-to-noise ratio of one, as presented in reference 2, using typical system coupling parameters. Where typical system performance specifications could be found, they were used. In digital systems, the 22-dB S/N requirement equates to an approximate bit error rate (ber) of 10^{-9}. All specifications have assumed a light-emitting diode (LED) as the optical source and a pin diode as the photodetector; low-loss (<10 dB/km) fiber optic cable has been used except where noted. These specifications are not exact and are intended only to represent the values for typical signal levels for these classes of systems.

The susceptibility levels for the analog and digital systems have not been considered in the same manner. For digital systems, the upset level was selected as that level which equaled one-half the received signal. This assumes a signal midpoint detection scheme. For radiation effects that cause permanent degradation, the loss of all the design margin was used. For analog systems, the susceptibility level was defined as that level which would increase the noise or reduce the signal sufficiently to produce a 3-dB decrease in the required S/N ratio, referenced to the typical received power. For fast transient responses, the perturbation of the system recovers very quickly, and therefore, this definition of susceptibility level for analog systems may be too conservative; however, this is a customary definition for analog systems and was used in the calculations.

---

[1] Vance, EF, Coupling to Shielded Cables, Wiley-Interscience, 1978

[2] AFAL TR-45, Opto-electronics Aspects of Avionic System II, by JR Baird, May 1975

System	Rate or Bandwidth	Power Required for Optimum Receiver (S/N = 1) (-dB m)	Typical Received Optical Power (-dB m)			Design Margin (dB)			Susceptibility Level (W)		
			<100 m	1 km	7 km	<100 m	1 km	7 km	<100 m	1 km	7 km
<u>Digital</u>											
Pt-pt	1 Mbps	63	21	31	35[a]	31	21	17	8×10^{6}	800×10^{-9}	320×10^{-9}
Pt-pt	10 Mbps	53	21	31	35[a]	21	11	7	8×10^{-6}	800×10^{-9}	320×10^{-9}
Pt-pt	100 Mbps	42	20	25[b]	–	11	6	–	10×10^{-6}	3.2×10^{-6}	–
Data bus	10 Mbps[b]	53	36	41[b]	–	6	1	–	250×10^{-9}	80×10^{-9}	–
<u>Analog</u>											
Video	5–10 MHz	57	21	31	35[a]	14	4	0	100×10^{-9}	10×10^{-9}	4×10^{-9}
Wideband	180 MHz	37	22	27[b]	–	5	0	–	1.25×10^{-6}	0.5×10^{-6}	–

[a]Requires fiber optic cables with <2 dB/km attenuation

[b]Requires fiber optic cables with <5 dB/km attenuation

Table 1. Electro-optic system performance parameters

To calculate the EMP vulnerability levels presented in table 2, it has been assumed that coupling and shielding loss from the incident power [$P_I(t)$] contained in the free-field pulse has been attenuated by 120 dB to the input of the fiber optic receiver. This level of attenuation was estimated as a level that could reasonably be obtained and maintained in the field. Of this, 60 dB is calculated for the coupling (dV/dt) from the capacitance of a typical detector package to the ground plane and 60 dB is allowed for the shielding effectiveness of the enclosure. The incident power in the EMP pulse has been defined as

$$P_I(t) = \frac{E(t)^2}{Z_0},$$

where

Z_0 = the impedance of free space (377 ohms)

$E(t)$ = the electrical free field.

The formula then used to calculate the magnitude of the free field is

$$|E(t)| = \left[Z_0\, P_{(threat)} \times \log^{-1} \frac{(\text{atten dB})}{10}\right]^{1/2}$$

$$\simeq 2 \times 10^7\, P^{1/2}_{(threat)} \text{ volts/meter,}$$

where $P_{(threat)}$ has been obtained from the susceptibility levels in table 1.

For systems that have an operate-through criterion, susceptibility to the prompt radiation pulse is of interest. Table 3 presents the prompt ionization dose rate susceptibility levels of fiber optic systems, calculated with the assumption that the dose rate radiation sensitivity is determined primarily by the response of the photodetector. This is warranted because the dose rates are very low and the prompt radiation pulse width is narrow. Therefore, the total ionization doses received by the links are very small, which would result in little fiber response. The prompt dose rate at which upsets in the link will occur have been calculated from the known response of one of the least radiation-sensitive pin diodes commercially available the HP 5082-4601, manufactured by Hewlett-Packard. This diode was radiation characterized (ref 3) and has an ionization dose rate (D) induced photocurrent (I_p) response of

$$I_p = 5.2 \times 10^{-10}\, \dot{D}.$$

The vulnerability level was defined as that radiation-induced photocurrent in photodetectors that would equal the normal optical signal-induced current generated at the susceptibility level (P_s) presented in table 1. The relationship used is

$$I_s = P_s \times R = I_p,$$

where

R = the responsivity of the pin diode (~0.5 A/W).

[3] Hardwick, WH, and Kalma, AH, Effects of Low-Dose-Rate Radiation on Opto-Electronic Components and the Consequences on Fiber Optic Data Link Performance, IEEE Trans Nucl Sci NS-26, No 6, December 1979

System	Rate or Bandwidth	Depth (m)	Length		
			<100 m	1 km	7 km
Digital					
Pt-pt	1 Mbps	0	55.0	17.0	11.0
		1	67.0	20.1	13.4
		2	81.8	25.3	16.4
		5	149.0	45.9	29.7
Pt-pt	10 Mbps	0	55.0	17.0	11.0
		1	17.0	20.1	13.4
		2	81.8	25.3	16.4
		5	149.	45.9	29.7
Pt-pt	100 Mbps	0	61.0	35.0	–
		1	79.4	42.7	–
		2	90.8	52.1	–
		5	165.0	94.5	–
Data bus	10 Mbps	0	10.0	5.0	–
		1	12.2	6.1	–
		2	14.9	7.4	–
		5	27.0	13.5	–
Analog					
Video	5-10 MHz	0	6.0	2.0	1.3
		1	7.3	2.4	1.6
		2	8.9	3.0	1.9
		5	16.2	5.4	3.5
Wideband	180 MHz	0	22.0	14.0	–
		1	26.8	17.1	–
		2	32.7	20.8	–
		5	59.4	37.8	–

Table 2. Electric free-field vulnerability levels (kV/m) for fiber optic data systems as a function of burial depth in the earth

System	Rate or Bandwidth	Depth (m)	Length <100m	1 km	7 km
Digital					
Pt-pt	1 Mpbs	0	7.7	0.8	0.3
		1	16.2×10^3	1.7×10^3	0.6×10^3
		2	34.0×10^6	3.5×10^6	1.3×10^6
		5	30.4×10^{15}	32.7×10^{15}	12.3×10^{15}
Pt-pt	10 Mbps	0	7.7	0.8	0.3
		1	16.2×10^3	1.7×10^3	0.6×10^3
		2	34.0×10^6	3.5×10^6	1.3×10^6
		5	314.0×10^{15}	32.7×10^{15}	12.3×10^{15}
Pt-pt	100 Mbps	0	0.6	3.1	–
		1	20.3×10^3	6.5×10^3	–
		2	42.3×10^6	13.7×10^6	–
		5	392.0×10^{15}	127.0×10^{15}	–
Data bus	10 Mbps	0	0.2	0.1	–
		1	420.0	210.0	–
		2	882.0×10^3	441.0×10^3	–
		5	8.2×10^{15}	4.1×10^{15}	–
Analog					
Video	5-10 MHz	0	0.1	0.01	0.003
		1	210.0	21.0	6.3
		2	441.0×10^3	44.1×10^3	13.3×10^3
		5	4.1×10^{12}	408.0×10^{12}	122.0×10^{12}
Wideband	180 MHz	0	1.3	0.1	–
		1	2.7×10^3	210.	–
		2	5.7×10^6	441.0×10^3	–
		5	53.1×10^{15}	4.1×10^{12}	–

Table 3. Prompt-dose-rate vulnerability levels [rd(Si)/s] at surface for fiber optic systems with an operate-through requirement as a function of burial depth in the earth

Therefore, the threshold ionization dose rate is

$$\dot{D} \simeq \frac{P_s R}{5.2 \times 10^{-10}} \simeq 10^9 \times P_s.$$

To determine the radiation level at which total dose accumulated at a low rate [<5 krd(Si)/s] will cause link performance degradation below the link design margin, three suppositions were made. First, the fiber response to the ionizing radiation environment has a dose rate ($\dot{D}$) dependence. This dose rate dependence has been reported (refs 3–6) for some of the most radiation-resistant fibers that have been tested. Second, the dose rate dependence of the fiber may be characterized as similar to those in reference 3. Finally, at a given dose rate, the induced attenuation is a linear function of the accumulated total dose (D_T) for total doses below 7 krd(Si). Using these assumptions and data from reference 6, the induced attenuation (A_I) at room temperature may be expressed as

$$A_I(\mathrm{dB/m}) = 3.27 \times 10^{-4}\, \dot{D}^{-0.56} \text{ for } D_T < 7 \text{ krd(Si) and } \dot{D} > 5 \text{ rd(Si)/s}.$$

Using this expression and the design margins (DM) presented in table 1, the formula for calculating the total dose needed to induce an attenuation equal to the design margin is

$$D_T = 3.06 \times 10^3\, \dot{D}^{0.44} \times \frac{DM}{\ell},$$

where

ℓ = the length of the fiber in metres.

For the levels presented in table 4, a dose rate of 8.3 rd(Si)/s was used; however, these levels would be valid for higher dose rates. For dose rates very much smaller than this value, the induced attenuation may not reach the design margin level, and therefore, the equation would be invalid. It should also be noted for this type of fiber that, once the radiation ceased, recovery would take place and the link would begin operating at some later time that would depend on the total dose received by the fiber and on its recovery rate.

Table 5 shows the increase in susceptibility level for total dose in a prompt pulse for these systems with several recovery times. The empirical equation developed to characterize the cable's (ITT 323) recovery from fast radiation pulses, as reported in reference 6, is

$$A_R = \ell(28 \times 10^{-3}) \log(t \times 10^5) + \ell K D_T \text{ for } t > 10^{-5} \text{ s}.$$

---

[4] ERADCOM TR-28-13, Nuclear Radiation Vulnerability of Proposed Army Fiber Optics Communications System, by S Kronenberg, et al, 1978

[5] Arimura, I, and Colwell, R, Radiation Degradation and Recovery in Long Fiber Optic Data Links, presented at 1980 Symposium on Fiber Optics in Nuclear Environment, March 25-27, 1980

[6] Sigel, GH, Jr, et al, Radiation Response of Large-Core Polymer-Clad Silica Optical Fibers, IEEE Trans Nucl Sci NS-26, No 6, December 1979

where

A_R = the amount of damage remaining in the cable (dB),

ℓ = the length of the cable (m),

t = the time period of recovery (s),

K = a constant that predicts the initial attenuation as a function of prompt total dose.

System	Rate or Bandwidth	Length <100 m	1 km	7 km
Digital				
Pt-pt	1 Mbps	2400	160	19
Pt-pt	10 Mbps	1630	85	8
Pt-pt	100 Mbps	854	47	–
Data bus	10 Mbps	466	8	–
Analog				
Video	5-10 MHz	1100	31	–
Wideband	180 MHz	388	–	–

Table 4. Low-dose-rate total-dose [rd(Si)] vulnerability levels for fiber optic systems

This cable has one of the lowest radiation-induced attenuations that have been reported. Even though it has a fairly low rate of recovery, it still has an induced attenuation that is below similar cables at the times used in the table. This formula may be combined with the performance specification to determine the total prompt dose (D_p) that may be sustained by the fiber and recover in the specified times presented in table 5. That is,

$$D_p = \frac{(DM + \ell)(28 \times 10^{-3}) \log(t \times 10^5)}{K\ell} \times 10^{d/3}.$$

Here, the last term in the expression has been used to allow for the attenuation of the ionizing radiation with the burial depth (d) in the earth, which was calculated for 1MeV photons to be a factor of 10 for ~0.3 m.

It should be noted that, for systems with longer recovery times, the susceptibility level is not strongly dependent on the design margin or on the length of the link. It is also interesting that, for any given depth, the prompt total dose vulnerability level for all the systems spans only one order of magnitude for this particular fiber optic cable.

Other environments of interest are those of natural space and steady state, such as that near a nuclear reactor. In these environments the opto-electronic components are subjected to constant fluxes of radiation particles (electrons, protons, gammas) that adversely affect operation of the data links (ref 3). The primary opto-electronic components that contribute to the degradation of operation of the data links are the fibers and the photodetectors. Using the same type of fiber that was used for the analysis above and the photodetector previously used, and assuming that the susceptibility level is that at which data

System	Rate or Bandwidth	Depth (m)	Length <100 m	1 km	7 km	Length <100 m	1 km	7 km	Length <100 m	1 km	7 km
			Recovery Time 1 ms			Recovery Time 1 s			Recovery Time 10 min		
Digital											
Pt-pt	1 Mbps	0	9.7×10^{3}	2.0×10^{3}	1.5×10^{3}	11.9×10^{3}	4.3×10^{3}	3.8×10^{3}	14.0×10^{3}	6.3×10^{3}	5.8×10^{3}
		1	20.3×10^{6}	4.3×10^{6}	3.2×10^{6}	2.5×10^{6}	8.9×10^{6}	7.9×10^{6}	29.3×10^{6}	13.2×10^{6}	12.2×10^{6}
		2	42.7×10^{9}	9.0×10^{9}	6.8×10^{9}	52.5×10^{9}	18.8×10^{9}	16.6×10^{9}	61.5×10^{9}	27.8×10^{9}	25.6×10^{9}
		5	400.0×10^{18}	80.0×10^{18}	60.0×10^{18}	500.0×10^{18}	200.0×10^{18}	200.0×10^{18}	570.0×10^{18}	260.0×10^{18}	240.0×10^{18}
Pt-pt	10 Mbps	0	7.0×10^{3}	1.8×10^{3}	1.5×10^{3}	9.3×10^{3}	4.0×10^{3}	3.7×10^{3}	11.3×10^{3}	6.0×10^{3}	5.8×10^{3}
		1	14.8×10^{6}	3.7×10^{6}	3.2×10^{6}	19.4×10^{6}	8.4×10^{6}	7.8×10^{6}	23.7×10^{6}	12.7×10^{6}	12.1×10^{6}
		2	31.0×10^{9}	7.8×10^{9}	6.6×10^{9}	40.8×10^{9}	17.6×10^{9}	16.4×10^{9}	49.8×10^{9}	26.7×10^{9}	25.5×10^{9}
		5	300.0×10^{18}	70.0×10^{18}	60.0×10^{18}	400.0×10^{18}	200.0×10^{18}	202.0×10^{18}	460.0×10^{18}	250.0×10^{18}	240.0×10^{18}
Pt-pt	100 Mbps	0	4.4×10^{3}	1.6×10^{3}	–	6.6×10^{3}	3.9×10^{3}	–	8.7×10^{3}	5.9×10^{3}	–
		1	9.2×10^{6}	3.4×10^{6}	–	13.9×10^{6}	81.0×10^{6}	–	18.2×10^{6}	12.4×10^{6}	–
		2	19.4×10^{9}	7.2×10^{9}	–	29.1×10^{9}	170.0×10^{9}	–	38.2×10^{9}	26.1×10^{9}	–
		5	200.0×10^{18}	70.0×10^{18}	–	300.0×10^{18}	200.0×10^{18}	–	350.0×10^{18}	240.0×10^{18}	–
Data bus	10 Mbps	0	2.3×10^{3}	1.5×10^{3}	–	4.5×10^{3}	3.7×10^{3}	–	6.5×10^{3}	5.8×10^{3}	–
		1	4.8×10^{6}	3.2×10^{6}	–	9.4×10^{6}	78.0×10^{6}	–	13.7×10^{6}	12.1×10^{6}	–
		2	10.0×10^{9}	6.6×10^{9}	–	19.8×10^{9}	164.0×10^{9}	–	28.9×10^{9}	25.5×10^{9}	–
		5	100.0×10^{18}	60.0×10^{18}	–	200.0×10^{18}	150.0×10^{18}	–	270.0×10^{18}	240.0×10^{18}	–
Analog											
Video	5-10 MHz	0	5.2×10^{3}	1.6×10^{3}	–	7.4×10^{3}	3.8×10^{3}	–	9.5×10^{3}	5.9×10^{3}	–
		1	10.9×10^{6}	3.3×10^{6}	–	15.5×10^{6}	8.0×10^{6}	–	19.9×10^{6}	12.3×10^{6}	–
		2	22.8×10^{9}	7.0×10^{9}	–	32.6×10^{9}	16.8×10^{9}	–	41.7×10^{9}	25.8×10^{9}	–
		5	202.0×10^{18}	60.0×10^{18}	–	300.0×10^{18}	160.0×10^{18}	–	390.0×10^{18}	240.0×10^{18}	–
Wideband	180 MHz	0	2.8×10^{3}	–	–	5.0×10^{3}	–	–	7.1×10^{3}	–	–
		1	5.9×10^{6}	–	–	10.5×10^{6}	–	–	14.9×10^{6}	–	–
		2	12.4×10^{9}	–	–	22.1×10^{9}	–	–	31.2×10^{9}	–	–
		5	100.0×10^{18}	–	–	210.0×10^{18}	–	–	290.0×10^{18}	–	–

Table 5. *Prompt total-dose vulnerability levels [rd(Si)] of fiber optic systems with allowances for recovery and depth of burial*

link operation will be degraded below the system specification levels, the degradation of the design margin is the sum of the fiber losses and the reduction of the S/N ratio of the link due to increased noise when these terms are expressed in decibels:

$$DM = \ell \times 3.27 \times 10^{-4}\, \dot{D}^{0.44} + 10 \log \frac{\dot{D}\, K_D^2}{I_n^2} + 1 \text{ (dB)},$$

where

ℓ = the length of the fiber (m),

k_D = the constant that relates the noise generated in the HP 5082-4601 photodetector = 2.02×10^{-9} A_{rms}/rd(Si)/s (ref 3),

I_n = the equivalent noise current at the input of the receiver calculated from table 6 optimum receiver power,

$$I_n = \log^{-1} \frac{(P_n \times R)}{10},$$

R = the responsivity of the photodetector.

The vulnerabilities for the fiber optic systems are given in table 6. It can be seen from the above equation, assuming equal dose rates on the detector and fiber, that for short cables the noise generated in the photodetector will cause link failure, whereas in long-distance links the induced attenuation in the fiber will cause the link to fail.

System	Rate or Bandwidth	Length		
		<100 m	1 km	7 km
Digital				
Pt-pt	1 Mbps	19	2	0.5
Pt-pt	10 Mbps	180	14	2.1
Pt-pt	100 Mbps	2200	200	
Data bus	10 Mbps	4.5	2.5	-
Analog				
Video	5-10 MHz	5.8	0.34	–
Wideband	180 MHz	3500	-	–

Table 6. Fiber optic system dose rate vulnerability levels [rd(Si)/s] for steady-state environments

HARD-WIRED DATA LINK RESPONSES TO RADIATION ENVIRONMENTS

For this portion of the report, the same six data systems have been analyzed for radiation susceptibilities. However, the frequency of operation of the data bus system has been lowered to 1 MHz. For the computations presented in the following tables, it is assumed that the links are interconnected with either twisted shielded pair (TSP) or coaxial cables that are terminated in their characteristic impedances. For those inter-

System	Rate or Bandwidth	Depth (m)	Burnout Length 10 m	Burnout Length 100 m	Burnout Length 1 km	Upset Length 10 m	Upset Length 100 m	Upset Length 1 km
Digital								
Pt-pt	1 Mbps	0	1.2×10^{9}	3.8×10^{8}	1.6×10^{9}[a]	1.7×10^{7}	5.4×10^{6}	2.2×10^{7}[a]
		1	2.6×10^{12}	8.1×10^{11}	3.3×10^{12}	3.6×10^{10}	1.1×10^{10}	4.7×10^{10}
		2	5.4×10^{15}	1.7×10^{15}	7.0×10^{15}	7.6×10^{13}	2.4×10^{13}	9.9×10^{13}
		5	5.0×10^{25}	1.6×10^{25}	6.5×10^{25}	7.0×10^{23}	2.2×10^{23}	9.1×10^{23}
Pt-pt	10 Mbps	0	1.2×10^{9}	3.8×10^{8}	1.6×10^{9}[a]	1.7×10^{7}	5.4×10^{6}	2.2×10^{7}[a]
		1	2.6×10^{12}	8.1×10^{11}	3.3×10^{12}	3.6×10^{10}	1.1×10^{10}	4.7×10^{10}
		2	5.4×10^{15}	1.7×10^{15}	7.0×10^{15}	7.6×10^{13}	2.4×10^{13}	9.9×10^{13}
		5	5.0×10^{25}	1.6×10^{25}	6.5×10^{25}	7.0×10^{23}	2.2×10^{23}	9.1×10^{23}
Pt-pt	100 Mbps	0	1.6×10^{10}[a]	5.0×10^{9}[a]	–	2.2×10^{8}[a]	7.1×10^{7}[a]	–
		1	3.3×10^{13}	1.0×10^{13}	–	4.7×10^{11}	1.5×10^{11}	–
		2	7.0×10^{16}	2.2×10^{16}	–	9.9×10^{14}	3.1×10^{14}	–
		5	6.5×10^{26}	2.0×10^{26}	–	9.1×10^{24}	2.9×10^{24}	–
Data bus	1 Mbps	0	1.2×10^{9}	3.8×10^{8}	–	1.7×10^{7}	5.4×10^{6}	–
		1	2.6×10^{12}	8.1×10^{11}	–	3.6×10^{10}	1.1×10^{10}	–
		2	5.4×10^{15}	1.7×10^{15}	–	7.6×10^{13}	2.4×10^{13}	–
		5	5.0×10^{25}	1.6×10^{25}	–	7.0×10^{23}	2.2×10^{23}	–
Analog								
Video	5-10 MHz	0	1.3×10^{10}[b]	4.1×10^{9}[b]	1.3×10^{9}[b]	8.2×10^{5}[b]	8.2×10^{4}[b]	1.6×10^{4}[b]
		1	2.7×10^{13}	8.6×10^{12}	2.7×10^{12}	1.7×10^{9}	1.7×10^{8}	3.4×10^{7}
		2	5.7×10^{16}	1.8×10^{16}	5.7×10^{15}	3.6×10^{12}	3.6×10^{11}	7.2×10^{10}
		5	5.3×10^{26}	1.7×10^{26}	5.3×10^{25}	3.3×10^{22}	3.3×10^{21}	6.7×10^{20}
Wideband	180 MHz	0	1.6×10^{10}[a]	5.0×10^{9}[a]	–	2.2×10^{8}[a]	7.1×10^{7}[a]	–
		1	3.3×10^{13}	1.0×10^{13}	–	4.7×10^{11}	1.5×10^{11}	–
		2	7.0×10^{16}	2.2×10^{16}	–	9.9×10^{14}	3.1×10^{14}	–
		5	6.5×10^{26}	2.0×10^{26}	–	9.1×10^{24}	2.9×10^{24}	–

[a]50-ohm coaxial systems
[b]75-ohm coaxial systems

Table 7. Dose rate vulnerability levels [rd(Si)/s] for buried hard-wired cables

System	Rate or Bandwidth	Depth (m)	Length 10 m	100 m	1 km	Length 10 m	100 m	1 km
<u>Digital</u>								
Pt-pt	1 Mbp	0	9.1	0.04	0.06[b]	0.13	0.5×10^{-3}	0.9×10^{-3}[b]
			(910)[a]	(3.7)	(6.3)	(13)	(0.05)	(0.09)
		1	11.1	4.5	7.7	0.16	0.06	0.11
			(1110)	(450)	(770)	(15.9)	(6.1)	(11)
		2	14.8	5.5	9.4	0.19	0.07	0.13
			(1480)	(550)	(940)	(19.3)	(7.4)	(13.4)
		5	24.5	10	17.0	0.35	0.13	0.24
			(2450)	(1000)	(1700)	(35.1)	(13.5)	(24.3)
Pt-pt	10 Mbps	0	9.1	0.06	0.06[b]	0.13	9×10^{-3}	0.9×10^{-3}[b]
			(910)	(6.3)	(6.3)	(13)	(0.09)	(0.09)
		1	11.1	7.7	7.7	0.16	0.11	0.11
			(1110)	(770)	(770)	(15.9)	(11)	(11)
		2	14.8	9.4	9.4	0.19	0.13	0.13
			(1480)	(940)	(940)	(19.3)	(13.4)	(13.4)
		5	24.5	17.0	17.0	0.35	0.24	0.24
			(2450)	(1700)	(1700)	(35.1)	(24.3)	(24.3)
Pt-pt	100 Mbps	0	15.8[b]	0.06[b]	–	0.22	9×10^{-3}	–
			(1580)	(6.3)	–	(22.5)	(0.09)	–
		1	19.3	7.7	–	0.27	0.11	–
			(1930)	(770)	–	(27.4)	(11)	–
		2	23.5	9.4	–	0.33	0.13	–
			(2350)	(940)	–	(33.5)	(13.4)	–
		5	42.7	17.0	–	0.61	0.24	–
			(4270)	(1700)	–	(60.8)	(24.3)	–
Data bus	10 Mbps	0	9.1	0.04	0.06[b]	0.13	0.5×10^{-3}	0.9×10^{-3}[b]
			(910)	(3.7)	(6.3)	(13)	(0.05)	(0.09)
		1	11.1	4.5	7.7	0.16	0.06	0.11
			(1110)	(450)	(770)	(15.9)	(6.1)	(11)
		2	14.8	5.5	9.4	0.19	0.07	0.13
			(1480)	(550)	(940)	(19.3)	(7.4)	(13.4)
		5	24.5	10	17.0	0.35	0.13	0.24
			(2450)	(1000)	(1700)	(35.1)	(13.5)	(24.3)

Table 8. Hard-wired cable EMP vulnerability levels (kV/m) as a function of depth of burial

Table 8 (cont)

System	Rate or Bandwidth	Depth (m)	Length			Length		
			10 m	100 m	1 km	10 m	100 m	1 km
Analog								
Video	5-10 MHz	0	13[c]	0.05[c]	0.05[c]	0.18[c]	7×10^{-3}[c]	5×10^{-3}[c]
			(1300)	(5.2)	(5.2)	(18)	(0.07)	(0.05)
		1	15.9	6.1	6.1	0.22	0.08	0.06
			(1590)	(610)	(610)	(22)	(8.5)	(6.1)
		2	19.3	74.4	74.4	0.27	0.1	0.07
			(1930)	(740)	(740)	(26.8)	(10.4)	(7.4)
		5	35.1	135	135	0.49	0.19	0.13
			(3510)	(1350)	(1350)	(48.6)	(18.9)	(13.5)
Wideband	180 MHz	0	15.8[b]	0.06[b]	–	0.22	9×10^{-3}	–
			(1580)	(6.3)	–	(22.5)	(0.09)	–
		1	19.3	7.7	–	0.27	0.11	–
			(1930)	(770)	–	(27.4)	(11)	–
		2	23.5	9.4	–	0.33	0.13	–
			(2350)	(940)	–	(33.5)	(13.4)	–
		5	42.7	17.0	–	0.61	0.24	–
			(4270)	(1700)	–	(60.8)	(24.3)	–
Multiplier for cable 10 m above ground (referenced to d = 0)			0.1	1.0	1.0	0.1	1.0	1.0

[a]( ) for cables with 80 dB S_E; all others 40 dB S_E

[b]50-ohm coaxial systems

[c]75-ohm coaxial systems

connected with TSP, the termination value of 150 ohms was used. The coaxial systems were assumed to be 50-ohm terminated except for the 5 to 10-MHz video system, which used 75 ohms for its termination. Further, no allowances were made for protection filters or surge suppression devices at the interface connections between the cables and the semiconductors. In the tables, the systems that use coaxial cables are identified with an asterisk. Cables were selected by considering the transmission rates or bandwidths and the lengths of cables.

Specific types of semiconductors that could be used in the implementation of the data links have not been considered for this report. It was assumed that standard IC technologies would be incorporated for both the digital and analog systems. It should be noted, however, that the 100-Mbps point-to-point digital link would probably have to be implemented with an IC technology similar to emitter-coupled logic (ECL, MECL, etc). The 180-MHz wideband link would probably be implemented using hybrid IC or discrete transistors. This is emphasized because the minimum burnout threshold for all the systems has been set at an energy level of 5×10^{-6} J. The range for the burnout threshold for specific devices covers approximately two orders of magnitude above this value, but it was decided that using this minimum-threshold value would result in a minimum susceptibility level and was, therefore, warranted in this study.

The upset levels for the analog and digital systems were again considered separately. For the digital systems, the upset energy threshold was set at 1×10^{-9} J. Interested readers who are unfamiliar with the concept of using energy to define both the burnout and upset levels, see reference 7 for a brief introductory discussion.

The upset levels for the analog systems have been set in the same manner as those in the fiber optic receivers. In fact, the same susceptibility levels were used in the calculations because the electrical power requirements for the hard-wired systems should be the same as those for fiber optic systems.

To calculate the ionization dose rates (table 7) that would create system-generated EMP (SGEMP) cable signals large enough to exceed the vulnerability thresholds of the semiconductors, the following assumptions were made. The energy (W_I) incident at the terminations of the cables could not exceed the threshold values. The energy at these points was defined as

$$W_I(t) = \int_0^t p(t)\,dt = \int_0^t e(t)\,i(t)\,dt = Z_0 \int_0^t i^2(t)\,dt$$

$$\simeq Z_0 I^2\, t_{(eff)},$$

where

p(t), e(t), and i(t) = the power, voltage, and currents, respectively, generated at the terminations as a function of time,

Z_0 = the cable termination impedance,

$t_{(eff)}$ = the electrical length of the cable.

---

[7] **NOSC Report TR-469, EMP Hardening of Airborne Systems through Electro-optical Techniques: Design Guideline, by R Greenwell, 15 December 1979**

The current function (I) used in this equation is the magnitude of current that would be generated in an effective length [$\ell_{(eff)}$] of the cable. The effective length of cable was defined as the velocity of propagation (v_{prop}) in the cable divided into the pulse width of the prompt pulse (t_{pw}). The resulting formula for the magnitude of the current is then

$$I = K\dot{D}\ell_{(eff)} = K\dot{D}\, t_{pw} \times v_{prop},$$

where

K = the generation constant for the cable (C/rd-cm),

$\dot{D}$ = the dose rate [rd(material)/s].

If the pulse width is expressed in nanoseconds and the velocity of propagation is ~0.25 m/ns, then

$$I = \frac{K\dot{D}}{4}\, t_{pw}.$$

It has been assumed that this current will flow for a period equal to the electrical length of the cable, and, therefore, the energy may be written as

$$W_I = I^2 Z\, t_{(eff)} = K^2 \dot{D}^2 \ell^2_{(eff)} Z\, t_{(eff)}$$

$$= \frac{K^2 \dot{D}^2 t_{pw}^2 \ell Z}{4}.$$

Solving the last equation for the dose rate yields

$$\dot{D} = \frac{6.32 \times 10^3}{Kt_{pw}} \sqrt{\frac{W_I}{\ell Z}},$$

where

t_{pw} = nanoseconds

ℓ = metres.

The attenuation (A_γ) of the radiation pulse through the soil may be taken into account by multiplying this expression by

$$A_\gamma \simeq 10^{d/0.3} \qquad (1\,\mathrm{MeV}, \gamma),$$

where

d = the depth of the soil in metres.

For the following, estimates of peak cable-shield currents induced by EMP are used as the starting point for various coupling calculations. This section describes the bases for those estimates.

A cable of 9.5×10^{-3}-m diameter and lengths of 10, 100, and 1000m was assumed. The cable was either 10 m above the ground, very near the ground, or 1, 2, and 5 m below

the ground surface. The ground conductivity was assumed to have a typical value of 10^{-2} mho/m. The driving EMP signal was the commonly used double exponential time history with roughly a 10-ns rise time and a 250-ns decay time. The direction of EMP incidence was chosen to give maximum cable currents.

In most cases the formulas used to estimate cable currents were taken from reference 1. (This book presents a good review of EMP coupling to long cables.) Infinite or semi-infinite cable theory was found to be generally applicable. For above-ground cables, the peak current saturates when cable lengths are longer than the drive pulse length times the speed of light (~76 m in this case). The semi-infinite cable formulas of reference 1 thus apply for the 100 and 1000-m cables. Note also that the finite ground conductivity (σ) makes the response of the cable near the ground larger than it would be near a perfect conductor.

For the 10-m cable above the ground, the formulas in reference 1 are not applicable. Estimates for this case were thus based on simple capacitive coupling ($I \sim C\dot{V}$). Note that this type of current estimate increases linearly with cable length and is thus invalid for the longer cables.

For buried cables, infinite cable theory is applicable for lengths greater than ℓ, where

$$\ell > 10^9\sqrt{\tau\,\tau_e}\,,$$

$$\tau = \text{pulse width} \simeq 250 \text{ ns},$$

$$t_e = \epsilon_0/\sigma \simeq 10^{-9} \text{ s}.$$

In this case $\ell \simeq 15$ m. Such theory was applied for all three cable lengths.

Note that characteristic current pulse widths correspond to the shorter of the drive pulse widths or to the cable length divided by the speed of propagation down the cable, ~0.25 ms.

The effects of soil attenuation have been taken into account by using 1 MHz as the mid-frequency of the energy contained in the double exponential pulse. The attenuation (A_S) is then

$$A_S = \exp[-d\sqrt{\pi f \mu_0 \sigma}] \simeq -d\,\frac{f_0}{503},$$

where

$$\mu_0 = 4\pi \times 10^{-7} \text{ H/m},$$

$$d = \text{depth in metres},$$

$$f = \text{frequency (Hz)},$$

$$\sigma = \text{ground conductivity (mho)}.$$

The magnitudes of the vulnerability levels, as presented in table 8, were then calculated from

$$|E|\,(\text{V/m}) = \frac{\log^{-1}\frac{SE}{10}}{K\,A_S}\sqrt{\frac{W_{threat}}{Z_{tpw}}}\,.$$

where S_E = shielding effectiveness of cables, 80 dB and 40 dB assumed,

K = peak current coupled onto cable (ref 8, p 86),

A_S = attenuation of the earth at the burial depth,

W_{threat} = energy level of the threat (5×10^{-6} J for burnout and 1×10^{-9} J for upset),

Z = termination impedance of the cable,

tpw = effective pulse width (250 ns for cables longer than 76 m and 40 ns for shorter cables).

RADIATION EFFECTS ON ELECTRONIC SYSTEMS

The radiation environments encountered by military systems are classified as nuclear-weapon-generated and natural (or space). These classifications may be further divided into components that produce basic effects on the electronics in the system. Many variations and combinations of the primary components of these two classifications exist and depend upon the particular system applications. The problem for the system designer is to achieve cost-effective and balanced hardening against all components of the particular radiation environment to ensure the survivability of the system. To accomplish this goal, he must be familiar with the primary components of the radiation environments and their effects on the system electronics. A brief description of the primary components of the two radiation environments, along with their basic effects, is presented in table 9 and the following discussion. The sources of the primary components in the radiation environments have been described in several documents, and are beyond the scope of this document.

The primary concern of system designers when hardening the system to radiation effects is for the semiconductors (integrated circuit and discrete) incorporated in most modern military systems, since they are the most vulnerable electronic components. This is not to say that there are no radiation effects in the passive components (eg, resistors, inductors, capacitors), but that they are typically less susceptible. However, in those military systems that must survive very severe radiation environments these components, especially electrolytic capacitors, must be included in the overall hardening effort.

The response of the system to the radiation environment may be categorized according to whether the effect is transient or permanent. In this case, "transient" and "permanent" refer to the effect produced by the radiation, not to the duration of the radiation environment. Transient effects in an electronic system may be produced by two primary components of the radiation environment: energetic particles penetrating the semiconductor materials, and EMP-generated signals coupled into the system. The first effect creates electron-hole pairs which produce photocurrents in the devices. This process results in ionization effects. The magnitude and duration of the effect depend on the number of ionizing particles that interact with the semiconductor material, its active volume, the number of electron-hole pairs created by each particle, and how long it takes them to either recombine in or exit the device. The observed response of an electronic circuit could range from an increase in circuit noise to large currents (10^{-3} to >10 A) flowing in the circuits.

Permanent changes within semiconductors may also be produced by many of the components of the radiation environment. These are usually categorized as bulk, surface, thermomechanical, and EMP-related effects. Bulk effects are produced by those constituents of the radiation environment (neutrons, protons, electrons, etc) that produce permanent

Radiation	Units	Basic Effect
Natural		
Electron fluence	e/cm^2	Ionization of surface material. Causes degradation, deterioration, charge buildup on satellite surface components.
Proton fluence	p/cm^2	Permanent degradation in solar cells and other directly exposed semiconductor devices.
Weapon		
X-ray		
Thermomechanical	cal/cm^2	Mechanical deterioration in form of spallation, glazing, cracking, weakening of mechanical integrity.
Ionization (prompt)	rd(Si)/s	Induced photocurrents cause transient upset and high currents in all electronics. Potential latchup of junction-isolated ICs.
Gamma-ray ionization (prompt)	rd(Si)/s	Same as X-ray prompt ionization effects.
Total ionizing dose	rd(Si)	Total accumulated ionizing radiation causes permanent changes in semiconductors. MOS is most susceptible.
Neutron fluence	n/cm^2	Permanent displacement in semiconductor material lattice structure, causing part degradation.
EMP and system-generated EMP (SGEMP)	V/m	SGEMP produced by X-ray environment. Both EMP and SGEMP induce currents in interconnecting cables, in antennas, and throughout a system.
Blast and shock		Creates overpressure that causes mechanical deformation and creates winds that pick up debris that can cause further damage.

Taken from reference 8

Table 9. Primary components of radiation environments

[8] IRT Report 4521-002, The ABC's of Radiation Hardening, April 1976

displacements within the crystalline structure of the semiconductor materials. The displacements will alter many of the parametric characteristics of the semiconductor devices such as forward current transfer ratio (h_{FE}), leakage currents, and capacitances.

The ionization components of the radiation environment may create permanent and transient parametric changes in the semiconductors. The principal permanent ionization effects are surface effects and burnout.

Surface effects are primarily due to trapped charges at or near the surfaces of the semiconductor active areas. Some parametric changes within semiconductor devices that may be caused by surface effects are in transconductance, capacitances, and leakage currents. If the ionization components of the radiation environment have sufficient magnitude to cause large current densities within the semiconductors, enough energy can be dissipated in the active areas of the devices to cause permanent parametric changes or, as a worst case, catastrophic failure (burnout).

The X-ray components of the radiation environment also may produce permanent effects on the system electronics. When low-energy X-rays are absorbed by a material, they deposit energy during the pulse in the form of heat. This creates a shock wave within the material, and if sufficient energy is released the stress buildup in the material will result in physical damage. The absorption and propagation of the energy is highly dependent on the material, but is usually larger in those materials with high atomic number (high Z). The heat produced may also be sufficient to cause spallation of the material.

A summary of the transient radiation effects in electronics is presented in figure 1, which shows a spectrum of typical nuclear effects on electronic systems for the neutron fluence, dose-rate, and total-dose environments. The impact of these effects on a system will depend heavily on the susceptibility of the circuit and its function. For example, in a missile application, the occurrence of an upset of a system may be critical to mission success, while in a satellite, a system upset could be nothing more than noise in the system.

Considerable attention has been given to system responses associated with the EMP threat from a nuclear weapons environment, since the incident fields generated by a single optimally positioned nuclear detonation may cover very large areas of the earth's surface. Systems that are most vulnerable to this threat are those that present large coupling volumes for the incident electromagnetic energy, such as hard-wired communication networks and aircraft. These systems, if not sufficiently protected, can couple enough electrical energy into the semiconductor piece parts to cause burnouts or upsets in those devices that directly interface with the hard-wired interconnections.

The coupling paths for fields external to the system are numerous. They include diffusion through the enclosure outer walls or leakage through penetrations, either deliberate or inadvertent. Deliberate penetrations include antennas, radars, and cable feedthroughs; inadvertent penetrations include doors, windows, bomb bays, and other apertures that are less obvious such as hydraulic lines and power-line pickups. In aircraft, this could occur through generators near air intakes, and, for permanent ground-based installations, the commercial power distribution networks.

The amount of electromagnetic leakage through various penetrations depends on the type of penetration and the total fields near the penetrations. Some penetrations are more sensitive to the local electric field, others to magnetic fields. Also, at some locations on the exterior, total electric fields will be large and magnetic fields small, while the opposite may be true elsewhere. This will depend on the geometry of the enclosure and its orien-

Neutron Effects (n/cm^2)		Dose-rate Effects [rd(Si)/s]		Total-dose Effects [rd(Si)]	
10^{15}	MOSFET degrades	10^{11}	Semiconductors saturated completely; currents unlimited	10^{6}	ECL degrades
	Hardened logic degrades				Some degradation in most semiconductors
10^{14}	TTL, RF, & FET transistors degrade	10^{10}		10^{5}	I^2L degraded, hardened CMOS & other MOS show degradation
	Most transistors & RTL/DTL degrade				Power transistors show degradation
10^{13}		10^{9}	Hardened logic threshold	10^{4}	Commercial PMOS/CMOS gate shifts
	Low-frequency transistors degrade		Transistors turned on hard		
10^{12}		10^{8}	Potential latchup condition	10^{3}	First commercial CMOS gate shifts
			Significant I_{pp}* in most semiconductors		
10^{11}	Power transistors degrade	10^{7}		10^{2}	Shift in quartz crystal frequency (∿2 ppm)
	SCR & UJT degrade		Photocurrent in PIN		
10^{10}		10^{6}		10^{1}	

*I_{pp} = Photocurrent magnitudes

Figure 1. Spectrum of radiation effects on semiconductor components and estimated susceptibility ranges (ref 1)

tation to the incident EMP and radiation.

For systems that are close enough to the detonation to receive significant photon energies, other EMP threats are generated within the system. These are system-generated EMP (SGEMP) and internal EMP (IEMP).

System-generated EMP is a result of the low-energy photon flux interacting with the external structural enclosures of the system. The low-energy photon interactions produce secondary-electron emission currents that create external surface currents and charge densities which contribute to the total external electric and magnetic fields. These total fields may then be coupled into the internal cables and circuits through the previously mentioned penetrations or apertures.

High-energy photons will penetrate t! ˙ external walls of the system and create secondary-electron emissions from the intern· ·faces of the enclosures and shielding components. The generated internal electrical and magnetic fields are then the source of the internal EMP threat. The magnitude of the generated fields is dependent on the incident photon flux and its spectrum, the size and shape of the enclosures, and the materials from which they are constructed.

In a ground based system near a nuclear attack, the source-region nuclear effects present formidable problems to the designer. A significant problem is the protection of equipment located at a sufficient distance to survive the direct attack but connected to long hard-wired cables in the vicinity of the detonation. Peak currents on the shields of these cables on the order of 100 kA that last for ~30 μs have been estimated by several theoreticians. For a typical 50-ohm coaxial cable with a shielding effectiveness of 80 dB, the energy on the center conductor at its terminations would be 15 mJ. Providing reasonable protection against this threat is difficult.

NUCLEAR VULNERABILITIES OF ELECTRO-OPTIC COMPONENTS

Electro-optic techniques can provide definite advantages to military systems over conventional techniques for gathering, storing, processing, and transmitting signals and data. Among electro-optic techniques is fiber optics technology. Proven benefits to the military of systems employing this technology include increased bandwidths, data rates, and transmission distances without repeaters, and various combinations of reduced weight and power consumption. Possible benefits, indicated by studies but not yet adequately demonstrated, include higher reliability, lower maintenance and life-cycle costs, longer mean time between failures, and greater EMP hardening.

It is the latter of these that has been the driving force for many radiation-hardening studies. The rationale for these studies has been that, since the fiber optic cable is immune to em radiation due to its dielectric nature, the system's hardness to EMP should be increased. This is logical for systems that consist of only fiber optic cables and are exposed to only the em energy components of the radiation environment. However, the real world requires that fiber optic systems have electronics (which are sensitive to the nuclear environment) associated with the cable, and relatively few military systems have only the em radiation as the total nuclear threat. Therefore, this section of the report presents a discussion of the response of fiber optic systems to the total radiation environment.

At the present state of development in fiber optic technology, lack of component standardization precludes easy interchange of the electro-optical components comprising the system. Therefore, when selecting these components, a system-level point of view must

be used; components may not be selected from just a radiation-hardness point of view because of the dependence of one component on another in overall system performance. The selection process is usually accomplished by a very long, complex, and iterative procedure that involves tradeoffs between optimum electro-optical performance parameters and optimum radiation hardness parameters. To aid in this procedure, the designer usually uses a link power or link loss budget, which may be a table or formula that presents the optical powers (or losses) at the electro-optical component interface points, along with the system requirements. The resultant calculated optical power, either excess or deficiency, is referred to as the design margin and is a measure of how well the system meets performance specifications.

The design margin may also be used as a measure of the system's radiation hardness to those effects that cause permanent or slow-recovery transient degradation in the component's operating parameters. However, use of only the design margin to predict transient-upset radiation hardness may lead to erroneous conclusions. Hardness to transient upset is dependent on both the design margin and the magnitude of received optical signals. The reason for this may be easily understood if one considers how the design margin may be increased — by increasing either receiver sensitivity or received optical power. Measures taken to increase receiver sensitivity will usually result in an increase in its radiation sensitivity which, in turn, results in a lower radiation-upset threshold. Therefore, from a radiation hardness point of view it is more advantageous to increase the system's received optical power, if possible. However, tradeoffs exist and other system design parameters, such as reliability and operating lifetime, may be adversely affected by methods taken to obtain the increase in optical power.

To enable the reader to understand the complexity of problems faced by the designer in selecting electro-optic components for use in a fiber optic system, a brief discussion of the pertinent radiation response of the components will be presented and tradeoffs affecting the overall design of the fiber optic system will be identified. For purposes of this discussion, the fiber optic system will be divided into seven sections — drivers, sources, connectors, fibers, detectors, amplifiers, and (for some systems) fiber optic couplers. Information presented here was taken from a report prepared for DNA under contract DNA001-76-C-0139 by IRT Corporation. The material contained in that report has been updated where new data were available.

DRIVERS

Electronic integrated and hybrid circuits designed specifically for driving solid-state light sources are being developed by some IC manufacturers. These circuits are intended primarily for digital applications. Some have been developed for the military under government contract, but no radiation-hardening requirements had been placed on them. Therefore, it is expected that these circuits will be no more radiation-resistant than the standard IC processing used in their construction. Fortunately, for most applications the speed of operation required to meet the electrical operating specifications for these circuits is high enough to require that high-frequency transistors be used in their construction. To obtain high-frequency response, manufacturers must use small-geometry, high f_t semiconductors in constructing the low-level signal-handling portions of these ICs. These areas are thus made less sensitive to the ionization components and the displacement damage-producing components of the radiation environments. However, the semiconductors that perform the buffer/driving function to the light source must handle much larger currents (10 – 200 mA) and, therefore, must have larger junction areas to reduce the power dissipation in the devices

and to increase thermal conductivity to the packages. The larger geometry presents larger radiation-sensitive volumes which will produce greater photocurrent responses and will probably set the upset levels for these devices.

Only one type of IC driver (SPX 3619, built by Spectronics, Inc) has been radiation-tested and reported in the literature (ref 9). The responses in a high-dose-rate, ionizing radiation environment indicated that the output transistors contributed to most of the photocurrent responses of the IC and that no significant (10%) permanent degradation occurred while in any of the radiation environments in which they were tested [~1 Mrd(Si) total dose from combined gamma, electron, and proton environments and 3×10^{12} n/cm^2 neutrons].

Primary radiation environmental concerns for the systems designer, over which he has no control, are whether the output drive current switching level and frequency response will degrade with accumulation of ionization total dose or with displacement damage-producing components of the radiation environments. Assuming that the light source is not an integral part of the driver circuitry, the designer may protect it from excessive drive currents produced in the driver IC when subjected to high-dose-rate ionization environments. This may be accomplished by using external current-limiting techniques such as resistors or active by-pass networks. A possible EMP vulnerability exists with these devices because they require electrical signals wired to their inputs and receive their power via the power supply bus. If these hard-wired connections couple enough energy into the device, burnouts or upsets will be induced within the devices. The sensitivity of these devices will be no greater than that of other devices developed by the same technologies. The range of thresholds will then be ~10 to 100 μJ for burnouts and ~1 to 10 nJ for upset levels (ref 10-12).

LIGHT SOURCES

This report treats only the two types of semiconductor light sources most likely to be used by the military in fiber optic communications systems. These are light-emitting diodes (LED) and laser diodes, both of which can be fabricated from many different III-V semiconductor materials to give somewhat different properties, primarily different emission wavelengths. The wavelength chosen must be compatible with the transmission properties of the fiber and ranges from 0.6 to ~1.3 μm. The tendency at present is toward development of sources that emit in the 1.0 to 1.3-μm range since some of the more promising fibers have lower optical attenuation and possibly less radiation response at these wavelengths.

---

[9] IRT Final Report for AFWL, Fiber Optic Radiation Test and Evaluation Program, Kirtland AFB, December 1978

[10] Motorola Application Note AN-707, Noise Immunity Comparison of CMOS vs Popular Bipolar Logic Families, by AA Allen, 1973

[11] Wunsch, DC, and Bell, RR, Determination of Threshold Failure Levels of Semiconductor Diodes and Transistors Due to Pulse Voltage, IEEE Trans Nucl Sci NS-17, 364 1970

[12] Tasca, DN, Pulse Power Failure Modes in Semiconductors, IEEE Trans Nucl Sci NS-17, 364, 1970

Alloy combinations such as InGaAs, InGaP, InGaAsP, and GaAlSnSb have been used to construct these emitters, but the most serious efforts are presently centered around InGaAsP. Another reason for this developmental trend is that the pulse dispersion of optical signals in the fibers is less at these wavelengths. This is significant because it makes possible longer transmission distances without repeaters at higher frequencies of operation.

The effects that radiation can have on optical sources and the general range of thresholds for observation of these effects are presented in table 10.

Degradation Level	Specific Effect	Optical Source	
		LED	Laser Diode
Catastrophic Damage	Ionization-induced burnout	10^{10} rd(Si)/s	10^{9} rd(Si)/s
	Electrical pulse burnout (100 ms)	50 - 3000 μJ	0.5 - 30 μJ
Transient Ionization Effects	Transient upset	3×19^{9} rd(Si)/s	10^{12} - 10^{13} rd(Si)/s
Permanent Degradation	Light output loss, ionization	10^{7} rd(Si)	10^{7} rd(Si)
	Light output loss, neutron	10^{12} - 10^{14} n/cm^2	10^{13} - 10^{15} n/cm^2
Thermomechanical Effects	Mechanical failure	1 cal/g(Au)	1 cal/g(Au)

Table 10. Damage thresholds of optical sources.

Catastrophic Damage

The ionization-induced threshold of 10^{10} rd(Si)/s for LEDs is a conservative figure since this was the maximum test level in the only experiments reported (ref 9,13) and only a few devices failed. The threshold may be lower for laser devices because they are operated at higher current densities and have smaller junction areas. The 10^{9} rd(Si)/s listed in table 10 is just a guess, but it is conservative since it is an order of magnitude lower than the LED threshold.

The electrical pulse burnout thresholds where the devices failed were measured directly in certain GaAs, GaP, and $GaAs_xP_{1-x}$ devices (ref 14). These devices generally are fast and, thus, are small-area devices . According to the Wunsch-Bell/Tasca model (ref 11,12) for burnout, the threshold is area-dependent, as was found to be true over the limited area range of the tested devices. Hence, the thresholds for the larger-area, high-power LEDs and the smaller-area laser diodes were scaled from the measured data by the area ratio. The GaP device tested has a large area and was a slow unit. Faster units of this type may have lower thresholds. The $Ga_xAl_{1-x}As$ LEDs were assumed to be similar to $GaAs_xP_{1-x}$ LED.

Laser diodes are small-area devices, and since the threshold is proportional to area, they are predicted to be more vulnerable than LEDs. Experimental information is almost

[13] AFWL TR-74-302, An Assessment of Fiber Optics Technology for Satellite Hardening, by AH Kalma, 1975

entirely lacking in this field, except for an operating-life test which showed that $Ga_xAl_{1-x}As$ cw devices fail at about 1 μJ for 100-ns pulses (ref 15). This agrees reasonably with the estimate in the table and reinforces its credibility. Since the estimated thresholds are low, this area is a very important one in which experimental information is needed.

Transient Ionization Effects

Transient upset causes a false signal that decays rapidly after the burst. There have been almost no studies of ionization-induced emission in LEDs or laser diodes. This is because the devices are operated at forward bias with high current densities, and photocurrents would be relatively less important. For estimation purposes, the photocurrent response of GaAs diodes is used. This value is $\sim 3 \times 10^{-9}$ (A/cm^2)/[rd(Si)/s] (ref 16). The predictions agree reasonably with results from the reported experiments on devices made from GaAs, GaP, $GaAs_xP_{1-x}$, and $Ga_xAl_{1-x}As$ (ref 3, 13).

Another transient ionization effect is the light produced by the steady-state ionization encountered in the space environment or by the delayed gammas from a prompt burst. In light sources this would produce a background light level which would be similar to added noise. This effect would remain while the radiation remained and disappear when the radiation was not present. There are no experimental data in this area; the numbers shown in the table are predictions from the photocurrent response relationship. Again, laser degradation thresholds are much higher than LED thresholds because of their higher operating current density.

Permanent Degradation

Permanent ionization effects are produced by the total ionizing dose absorbed by a device. Surfaces or interfaces are affected primarily through increased leakage current, with some change in capacitance. The light sources are essentially unaffected by leakage current, and no ionization mechanisms (as opposed to displacement damage mechanism) have been reported (ref 3, 17, 18). Even though it is displacement damage that causes the degradation, most studies were performed with gamma fluence (ref 19-28), so this is how the thresholds are shown in table 10.

Displacement effects in the light sources produce competing nonradiative recombination centers and degrade the light output of the LEDs. In laser diodes a more important process is the lasing threshold shift. Lasers operated well above threshold will not show much degradation at low fluences. Eventually, the threshold shifts enough that the output drops drastically. The fluence required for this to occur in devices operated at a power factor of 3 from the maximum is considered the threshold.

The thresholds shown in table 10 are taken from a large number of studies (ref 23-42). The range of thresholds is apparently due to varying device quality, with the better-quality devices being more vulnerable. The better-quality devices have higher efficiency and, thus, fewer initial nonradiative recombination centers; therefore, it requires a lower radiation fluence to introduce a comparable number of new centers.

14–42 (see p 28, 29)

[14] Kalma, AH, and Fisher, W, Electrical Pulse Burnout Testing of Light-Emitting Diodes, IEEE Trans Nucl Sci NS-22, 2510, 1975

[15] O'Brien, JT, et al, Recent Developments in Injection Lasers, presented at Conference on Laser and Electro-Optical Systems, San Diego, California, 25-27 May, 1976

[16] AFWL TR-68-31, vol 2, Radiation Effects on GaAs Devices and Schottky Diodes, by HD Southward and RH Schnurr, August 1968

[17] Northrop Report DNA3776F, Study of Radiation Effects in Bulk CMOS Microcircuits, IIL/LSI Logic Cells, and Optic Couplers, by JP Raymond, et al, 1975

[18] Barnes, CE, Development of Efficient Radiation-Insensitive GaA:Zn LEDs, IEEE Trans Nucl Sci NS-24, No. 6, December 1977

[19] AFAL TR-74-61, Survey of Vulnerability of Contemporary Semiconductor Components to Nuclear Radiation, by RP Donovan, et al, 1974

[20] Epstein, AS, et al, Gamma Irradiation and Annealing Effects in Nitrogen-Doped GaAsP Green and Yellow Light-Emitting Diodes, IEEE Trans Nucl Sci NS-19, 386, 1972

[21] Barnes, CE, Effects of ^{60}Co Gamma Irradiation on Epitaxial GaAs Laser Diodes, Phys Rev B1, 4735, 1970

[22] Schnurr, RH, and Southward, HD, Radiation Effects on GaAs Devices, IEEE Trans Nucl Sci NS-15, 306, 1968

[23] Soda, KJ, et al, The Effect of Gamma Irradiation on Optical Isolators, IEEE Trans Nucl Sci NS-22, 2475, 1975

[24] Polimadei, RA, et al, Performance of GaAlAs Light-Emitting Diodes in Radiation Environments, IEEE Trans Nucl Sci NS-21, 96, 1974

[25] Share, S, et al, Radiation Effects and Hardening on Compensated GaAs Light-Emitting Diodes, IEEE Trans Nucl Sci NS-20, 256, 1973

[26] Epstein, AS, et al, Radiation Effects on Active and Passive Optical Components, presented at DoD/Industry-Wide Integrated Optics and Fiber Optics Communications Conference, NELC, San Diego, California, 1974

[27] Schroeder, JD, et al, Radiation-Damage-Induced Time Delay in GaAs Lasers, IEEE Trans Nucl Sci NS-19, 391, 1972

[28] Epstein, AS, and Trimmer, PA, Radiation Damage and Annealing Effects on Photon-Coupled Isolators, IEEE Trans Nucl Sci NS-19, 391, 1972

[29] Barnes, CE, Radiation Effects in Electroluminescent Diodes, IEEE Trans Nucl Sci NS-18, 322, 1971

[30] Noel, BW, et al, Neutron Irradiation Effects on Diffused GaAs Laser Diodes, IEEE Trans Nucl Sci NS-18, 378, 1971

[31] Barnes, CE, Neutron Damage in Epitaxial GaAs Laser Diodes, J Appl Phys 42, 1941, 1971

[32] Schade, H, et al, Defect Centers in GaAsP Electroluminescent Diodes Due to High-Energy Electron Irradiation, J Appl Phys 41, 3783, 1970

The $Ga_xAl_{1-x}As$ devices are relatively new and have not been heavily tested. Where they have been (ref 3), they appear to be comparable to $GaAs_xP_{1-x}$ devices, and both these types seem to be an order of magnitude harder than GaAs devices. In fact, use of ternary compounds to fabricate devices has been proposed as a hardening technique (ref 18,25,26). At times, the limited testing of the ternary material devices has produced degradation thresholds only at one end of the expected range. Some early GaAs work indicated neutron degradation thresholds higher than those listed in the table. The tested devices probably were of lower quality than those currently available, and this resulted in their being less vulnerable.

Thermomechanical Effects

No data exist concerning thermomechanical damage in light sources. The thresholds listed in table 10 assume that the light sources behave similarly to silicon semiconductor devices. This means that the contact bonds are the most vulnerable point of the devices. The light sources will almost assuredly be protected from the direct X-ray beam, so it is unlikely that any of the damaging low-energy X-rays would reach them.

CABLES

Table 11 presents the damage thresholds for fibers. Almost all effects depend on fiber length, so the thresholds are quoted per unit length. To calculate the thresholds, it has been assumed that in most receivers the noise level would be equivalent to an input signal of a few nanowatts. Thus, the minimum signal required for a 20 dB S/N ratio would be about 100 nW, and this is assumed to be the conservative signal leaving the fiber.

---

[33] Barnes, CE, Neutron Damage in GaAs Laser Diodes at and above Laser Threshold, IEEE Trans Nucl Sci NS-19, 382, 1972

[34] Epstein, AS, et al, Effect of Neutron Irradiation on GaAsP Electroluminescent Diodes, Appl Phys Lett 23, 472, 1973

[35] Stanley, AG, Comparison of Light-Emitting Diodes in a Space Radiation Environment, IEEE Trans Nucl Sci NS-17, 239, 1970

[36] Sandia Report SC-RR-710686 Radiation Effects in Light-Emitting Diodes and Laser Diodes, by CE Barnes, 1972

[37] Barnes, CE, Neutron Damage in GaP Light-Emitting Diodes, Appl Phys Lett 20, 110, 1972

[38] Compton, DMJ, and Cesena, RA, Mechanism of Radiation Effects on Lasers, IEEE Trans Nucl Sci NS-14, 55, 1967

[39] Arnold, GW, Luminescence in Intrinsic and Annealed Electron-Irradiated GaAs:Cd, Phys Rev 183, 777, 1969

[40] Barnes, CE, Appl Phys Lett 20, 86, 1972

[41] Barnes, CE, Tunneling in SiC Electroluminescent Diodes, J Appl Phys 45, 193, 1974

[42] Barnes, CE, Increased Radiation Hardness of GaAs Laser Diodes at High Current Densities, J Appl Phys 45, 3485, 1974

Degradation Level	Specific Effect	Special Glass-Clad Silica Fibers	Polymer-Clad Silica Fibers	Plastic Fibers
Transient Ionization Effects	Transient upset signal	10^6 - 10^8 rd(Si)/s-m	10^4 - 10^6 rd(Si)/s-m	10^4 - 10^5 rd(Si)/s-m
	Transient signal loss (immediate)	10^{10} rd(Si)/s-m	3×10^{10} rd(Si)/s-m	3×10^{10} rd(Si)/s-m
	Transient signal loss (1 ms)	10^9 - 10^{11} rd(Si)/s-m	3×10^{11} rd(Si)/s-m	10^{11} - 10^{12} rd(Si)/s-m
Permanent Degradation	Ionization-induced signal loss	10^0 - 10^3 rd(Si)/s-m	10^0 - 10^3 rd(Si)/s-m	10^5 - 10^7 rd(Si)/s-m
Thermomechanical Effects	Mechanical failure	10 cal/g(Au)	10 cal/g(Au)	10 cal/g(Au)

Table 11. Damage thresholds of fibers

Catastrophic Damage

Optical fibers, having no junctions, are immune to this effect. They are also immune to electromagnetic pickup, and therefore, do not produce electrical pulses capable of burning out other components. This is the primary reason that fiber optic systems are considered for radiation hardening.

Transient Ionization Effects

Transient ionization effects are the most important radiation vulnerability mechanisms in fibers, and most of the studies of radiation effects in fibers have examined this point (ref 43-60).

---

[43] Evans, BD, and Sigel, GH, Jr, Radiation-Resistant Fiber Optic Materials and Waveguides, IEEE Trans Nucl Sci NS-22, 2462, 1975

[44] Mattern, PL, et al, Effects of Radiation on Absorption and Luminescence of Fiber Optic Waveguides and Materials, IEEE Trans Nucl Sci NS-21, 81, 1974

[45] Evans, BD, and Sigel, GH, Jr, Permanent and Transient Radiation-Induced Losses in Optical Fibers, IEEE Trans Nucl Sci NS-21, 113, 1974

[46] NRL Memorandum Report 2704, Radiation Effects in Fiber Optic Waveguides, by GH Sigel, Jr, 1973

[47] Mattern, PL, Radiation-Induced Absorption and Luminescence in Glass and Plastic Optical Waveguides, presented at DoD/Industry-Wide Integrated Optics and Fiber Optics Communications Conference, NELC, San Diego, California, 1974

[48] NRL Memorandum Report 2934, Radiation Effects in Fiber Optic Waveguides, by GH Sigel, Jr, et al, 1974

Two transient effects in fibers can be produced by ionization. One is luminescence, which would produce an upset signal. The second is an increase in attenuation. The latter is the most important radiation effect in fibers because it decays slowly with time following exposure. Slow decay means that the transmission capability of a link will be lost not only during exposure but possibly for a long period following exposure. The thresholds shown in table 11 assume a 100-ns pulse width. This arbitrary choice is in the area of pulse widths at which exposure may occur. Scaling to other pulse widths should be done by the ratio of pulse widths.

The initial high absorption can produce a transient loss of signal if the dose is high enough. The threshold depends on the time interval after the burst that is required for the system to return to operation. The thresholds shown are for continuous operation ("immediate"), for operation 1 ms after the burst, and for operation 1s after the burst. These times are arbitrarily chosen to show how the threshold is affected. Recovery of the plastic fibers takes longer in a vacuum than in room-ambient conditions, apparently because of some atmospheric constituent (probably oxygen) scavenging the absorption centers (ref 50,52-54). The range of thresholds shown for transient upset signal depends on whether the data were measured using X-rays or low-energy electrons, with electrons providing the lower threshold.

---

[49] AFCRL-TR-74-0012, Transient Radiation Effects Tests of a Corning Radiation-Resistant Optical Fiber, by JA Wall, 1975

[50] AFCRL-TR-75-0190, Radiation Effects on Fiber Optics, by JA Wall and JF Bryant, 1975

[51] Mattern, PL, et al, Effects of Radiation on Optical Fibers and Materials, IEEE Trans Nucl Sci NS-22, 2468, 1975

[52] Sandia Report SAND76-8056, A Summary of Radiation-Induced Transient Absorption and Recovery in Fiber Optic Waveguides, by CD Skoog, 1976

[53] IRT Report INTEL-RT 8111-089, Fiber Optics Test Program for Satellite Applications, by AH Kalma and WH Hardwick

[54] Kalma, AW and Hardwick, WH, Radiation Testing of a Fiber Optics Data Link, IEEE Trans Nucl Sci NS-23, 1769, 1976

[55] Maurer, RD, et al, Effect of Neutron and Gamma Radiation on Glass Optical Waveguides, Appl Opt 12, 2024, 1973

[56] Sigel, GH, Jr, and Evans, BD, Effects of Ionizing Radiation on Transmission of Optical Fibers, Appl. Phys Lett 24, 410, 1974

[57] Acharekar, MA, Multimode Radiation-Resistant Glass Fiber for Data Transmission Applications, presented at DoD/Industry-Wide Integrated Optics and Fiber Optics Communications Conference, NELC, San Diego, California, 1974

[58] Sigel, GH, Jr, Radiation Damage in Fiber Optics, presented at DoD/Industry-Wide Integrated Optics and Fiber Optics Communications Conference, NELC, San Diego, California, 1974

[59] Friebele, EJ, et al, Radiation Protection of Fiber Optics Materials: Effects of Oxidation and Reduction, Appl Phys Lett 24, 412, 1974

[60] Friebele, EJ, et al, Defect Centers in a Germanium-Doped Silica-Core Optical Fiber, J Appl Phys 45, 3424, 1974

Steady-state transient effects in fibers are much the same as the above pulse effects. These could be produced by either delayed gammas or space electrons, both of which produce ionization for much longer periods of times than the prompt pulse, hence, the term "steady state". The most important effect is signal loss which does not occur at the same dose rate as for prompt transient pulses because recovery is occurring at the same time as generation. To predict the amount of attenuation produced by a steady state environment it is necessary to combine the production rate and the recovery rate, with the time elapsed since any exposure increment (ref 3-6, 50, 53, 54). The threshold depends on the exposure time and the magnitude of the steady state flux. The thresholds shown in the table assume a 10-s exposure to a constant flux, and require that the attenuation be low enough for link operation at the end of this period. Some data exist on the steady state response of fibers (ref 3-6,53,54), but none on the performance of a fiber optic system; therefore, the thresholds are the result of calculations.

A second effect of a steady state environment is the increased noise due to increased background light, which would be the result of luminescence. The increased noise could degrade the available S/N level of a fiber optic link, but it has not been reported.

Permanent Degration

The ionization-induced permanent degradation is the increase in fiber absorption which decreases the transmitted signal (ref 13,43-60). The absorption is the same effect as the transient absorption described above. Although the increased absorption decays indefinitely, the portion considered permanent degradation is that present one or two days after exposure.

Displacement damage cannot be measured in the fibers because the accompanying ionization produces more damage than displacement does (ref 13,43,49-52,55). The fibers are, for the purposes of this study, immune to displacement damage.

Thermomechanical Effects

The most likely effect of thermomechanical damage in fibers is surface cracking produced by the heating (ref 61) and this is the threshold shown. It is a higher threshold than for similar effects in devices because there are no wire bonds in the fibers; these bonds are the weak points. Another effect in the fibers could be dielectric breakdown caused by fiber charging. Calculations indicate that the threshold for breakdown is of the same order of magnitude as that for cracking caused by heating in the extreme case of using a gold converter, assuming that all the electrons are absorbed at the surface of a plane of fiber material with no leakage. Since this is worse than would occur in practice, dielectric breakdown would probably not be a vulnerability problem for an X-ray threat. However, for the natural or weapon-enhanced space environments this could be a problem.

---

[61] Baba, A, et al, Effect of Simulated Nuclear Thermal Pulses on Fiber Optic Cables, IEEE Trans Nucl Sci NS-26, No 6, December 1979

DETECTORS

Limited studies (ref 4,62) of the radiation effects in photodetectors have been made, but not with any degree of completeness, and unfortunately many of the threshold levels must be inferred. The information is summarized in table 12.

In determining upset and noise thresholds, some knowledge of the input light level and system operation, including system noise and bandwidth, is required. On the pessimistic side, it is assumed that the noise level is not set by the photodetector itself but by the amplifier, where the noise is about an order of magnitude higher in well designed systems. System bandwidth would also be somewhat less. Therefore, the listed thresholds of diode devices are low by at least this order of magnitude in systems using currently available electronics. However, improvements could lower the noise of the electronics and make the detector noise more important. Thus, the listed thresholds are minimum ones for a system that may be approached in the future.

Degradation Level	Specific Effect	Pin Diode	Avalanche Photodiode
Catastrophic Damage	Ionization-induced burnout	10^9 rd(Si)/s	10^9rd(Si)/s
	Electrical pulse burnout (100 ns)	100-40,000 μJ	200-4,000 μJ
Transient Ionization Effects	Transient upset	1-100 rd(Si)/s	0.01-1 rd(Si)/s
Permanent Degradation	Ionization-induced response degradation	$>10^8$ rd(Si)	$>10^8$ rd(Si)
	Ionization-induced dark current increase	10^4-10^6 rd(Si)	10^4-10^6 rd(Si)
	Neutron-induced response degradation	$10^{13}-10^{14}$ n/cm^2	$10^{13}-10^{14}$ n/cm^2
	Neutron-induced dark current increase	$10^{10}-10^{13}$ n/cm^2	$10^{10}-10^{14}$ n/cm^2
	Electron-induced response degradation	$10^{14}-10^{15}$ e/cm^2	$10^{14}-10^{15}$ e/cm^2
	Electron-induced dark current increase	$10^{11}-10^{14}$ e/cm^2	$10^{11}-10^{14}$ e/cm^2
Thermomechanical Effects	Mechanical failure	1 cal/g(Au)	1 cal/g(Au)

Table 12. Damage threshold of photodetectors

[62] Radiation Testing of Photodetectors, Final Report Contract F29601-76-C-0034, by WH Hardwick and AH Kalma, February 1978

Catastrophic Damage

This is an area in which essentially no work on photodetectors has been performed, but the similarity of photodetectors to other silicon devices can be used to estimate thresholds (ref 17,19,63-65).

For ionization-induced burnout, sensitive silicon devices are damaged at 10^9 rd(Si)/s, so this is taken as the threshold. For electrical pulse burnout, all silicon junction devices behave similarly, and their thresholds can be calculated by the Wunsch-Bell/Tasca model of junction burnout (ref 11, 12). In this model the thresholds depend on the semiconductor junction area (which is not necessarily the active optical area of a photodetector), allowing results for other devices to be scaled by the area ratio. The question that arises in scaling photodetector data is that their junction areas are larger than those of normal devices, and the burnout area may be less than 1/10 of the junction area assumed by the model. This would mean that the formula overestimates the threshold. To allow for this possibility, the estimates shown in table 12 are 10 percent of the scaled values so as to be pessimistic. The range of thresholds shown for any device type is caused by the range of device sizes.

However, it has been calculated (ref 66) that the fields in the depletion region of a pin photodetector will begin to collapse at dose rates of 10^7 rd(Si)/s; the radiation-induced photocurrents will tend to saturate at levels above this threshold and the recovery times will become longer with increasing dose rates.

The ionization-induced burnout mechanisms of these devices are the same as for normal silicon devices, and hardening by normal techniques (eg, current limiting) can be used on them. For all but the smallest devices, the electrical pulse burnout thresholds are high. However, the thresholds are only estimates which are uncertain, even by the low accuracy of burnout threshold standards. Therefore, the greatest need in this area is an experimental investigation of the thresholds so that the area can be properly assessed.

Transient Ionization Effects

Photodetectors are designed to be very sensitive to optical radiation. As a result, they are also very sensitive to radiation ionization, a similar phenomenon. Taking the definition of a rad and converting the energy deposited into electron-hole pair current in silicon, the theoretical current produced in devices without gain is

$$I = 6.4 \times 10^{-6} V\dot{\gamma},$$

where

I = amperes
V = the volume in cm^3,

and

$\dot{\gamma}$ is the dose rate in rd(Si)/s.

---

[63] DNA 1420H-1 TREE Handbook vol 1 by RK Thatcher, 1971

[64] HDL DS-94-1, Radiation Effects on Semiconductor Devices Summary Report, Components Response Information Center (DNA Data Bank), June 1974

[65] Gulf RT C12375, Status of Integrated Circuits, by LD Cotter and MA Donaldson, November 1975

[66] Gwyn, CW, Analysis of Radiation Effects in Semiconductor Junction Devices, IEEE Trans Nucl Sci NS-14, No 6, December 1967

Data on pin diodes used as ionization detectors and the (sparse) experimental information available on detectors (ref 16,17,28) tend to substantiate this theoretical value. For devices with gain, the gain multiplies the current determined in this manner.

The limited bandwidth of photovoltaic and transistor devices and their fast roll-off (~100 ns) increase the threshold. The larger-area devices are somewhat more sensitive, which is why the smaller pin diodes and avalanche photodiodes show higher thresholds than the other diode devices.

All of these transient upset thresholds are low. However, since they are directly related to the optical detection ability of the devices, little can be done to increase them except to change the material from which the detector is constructed. The smallest detector possible should be used to minimize the response, and the band-width narrowed to roll off the fast ionization response. Also, the signal-to-noise ratio should be made as high as possible by increasing the optical signal, thus requiring a larger upset pulse. This indicates that over-optimization of the receiver to reduce the noise and thus increase the S/N ratio should be avoided because it could make the system more vulnerable to upset. Obviously, shielding also decreases the vulnerability.

Steady-state noise increase is similar to transient ionization upset in that the former effect is produced by the current attributable to the latter. The difference is that steady-state effects are produced by a continually present source of ionization, such as the space-electron environment or a delayed-gamma environment. The primary effect of the steady-state ionization is to increase the noise current in the photodetector. Once the ionization ceases, the steady-state ionization effects will cease as well, so they are actually transient.

In principle, the radiation noise current may be calculated in the same manner as the transient upset signal, since the calculated radiation-induced noise current is the same type of "white" noise as the "dark" current noise. However, in these calculations the average current produced per penetrating ionization particle must be taken into account. Each type of ionization particle produces different amounts of electron-hole pairs, and, therefore, the average current per event is different for different particle fluxes. But the rms value for the radiation-induced noise current scales as the square root of the dose rate in the material, independent of the radiation particle (ref 3). The threshold is independent of system bandwidth for all but the photovoltaic types, where a maximum system bandwidth is assumed. These calculations produce thresholds which agree reasonably with those found in the few experiments that have been performed on pin photodiodes (ref 53,54,67,68).

As in the case of transient upset vulnerability, the steady-state ionization vulnerability cannot be usefully lessened in a given material by material property changes because it is related to optical sensitivity. However, switching to completely different semiconductor materials such as GaAs may raise the threshold because the generation rate in the materials may be reduced due to larger bandgaps. In fact, some of these detectors are being developed for the longer-wavelength LEDs, and these may have a higher threshold.

---

[67] IRT Report INTEL RT 0040-001, Test of MIRIS Radiometer Detectors, by AH Kalma, August 1976

[68] IRT Report INTEL RT 0039-001, Irradiation Testing of Optics Components, by AH Kalma and RA Cesena

Permanent Degradation

Permanent ionization or displacement effects could increase the device surface leakage and thus the noise, or degrade the device gain and thus the optical response. Unfortunately, very little data exist in the area of noise increase (ref 3,53,68), and only little more in the area of responsivity degradation (ref 28,53,54), and most of these are for pin photodiodes. Estimates of the vulnerability of the other device types are made from knowledge of similar effects in normal silicon devices (ref 17,19,63,65,67). All of the diode devices except the photovoltaic cells are usually biased to depletion, which means that the response is governed by carrier sweepout and not lifetime, so they should be relatively hard to displacement damage. The photovoltaic cells should be similar in vulnerability to solar cells because both are unbiased "ON" junction devices. The phototransistors should be similar to other transistor devices. In most cases, the thresholds are only estimates with little or no experimental justification.

The dark-current changes are likely to be dependent on device geometry and construction, and it is very difficult to estimate damage thresholds. Therefore, the numbers in the table have a very large range. This is not true for electron effects on photovoltaic cells, based on data from a silicon vidicon tube (ref 69) and solar cell experiments (ref 70). An experiment examined changes in dark current in large-area pin diodes and found increases of about a factor of 3 to 5 after 1.3×10^{11} n/cm^2 (ref 53). Since large-area devices are likely to be most vulnerable, this threshold supports the estimates.

Thermomechanical Effects

Since photodetectors will probably be protected from the direct X-ray beam, it is unlikely that they will suffer thermomechanical damage. The most vulnerable point of the devices will be the wire bonds; the listed thresholds are those determined for devices without wire bonds.

RECEIVERS

Because of the very low-level signals produced in the photodetectors, amplification of these signals is necessary before any further signal processing can take place. This is usually accomplished in several stages of specially designed amplifiers. However, the first stages are most critical because most of the receiver's performance parameters are attained there. The first stages are designed to transform the nanoamperes of optically generated photocurrents in the detector to voltage levels on the order of 50 to 200 millivolts while adding as little distortion and noise as possible. Therefore, these stages are required to have high gain at low currents, low noise, and usually high frequency response. These requirements place restrictions on the semiconductors that may be employed to implement the amplifiers; therefore, some basic predictions of the radiation responses of the amplifiers are possible even though no specific design is being analyzed.

---

[69] Brucker, GJ, and Cope, AD, Radiation Sensitivity of Silicon Imaging Sensors on Missions to the Outer Planets, IEEE Trans Nucl Sci NS-19, 147, 1972

[70] Jet Propulsion Laboratory Report 21945-6001-RV-00, Solar Cell Radiation Handbook, by JR Carter, Jr. and HY Tada, June 1973

The sensitivity of the amplifiers makes them very susceptible to any radiated em energies, which means that upsets in EMP environments should occur at much lower levels unless the amplifiers are heavily shielded. Burnout is not expected to be a problem since the only electrical connections are to the power supplies and the signal output. The power supply leads are easily filtered, and the outputs should not have long cables connected to them.

In the dose-rate environment, providing high threshold levels for upsets is expected to be difficult because of the high gain requirements of the amplifiers. Radiation-generated photocurrents within the semiconductors, unless they are fully compensated, should be larger than the signal levels at moderate dose rates, $\sim 10^5$ to 10^6 rd(Si)/s. However, they should not be as sensitive as the photodetectors because the semiconductors would have smaller radiation-sensitive volumes. Similarly, in the steady-state radiation environments, ionization-induced noise will decrease the S/N ratio, but this decrease is again not expected to be as large as that in the photodetectors.

Recovery of these amplifiers from the neutron flux will require a longer time because of the lower operating currents. The short-term annealing does not recover as rapidly at these levels (<1 μA) as it does in the milliampere range.

The total-dose components and those which produce displacement damage are also expected to present a problem for these amplifiers. The low quiescent operating currents required by the stages will be very sensitive to increases in leakage currents, and the high gain requirements will be sensitive to gain degradation. However, some designs for the amplifiers (transimpedance) use large amount of feedback and should, therefore, compensate for some of these effects.

Few of these devices are available from the IC manufacturers, but more should become available in the near future. One, the TIEF 151 preamplifier, manufactured by Texas Instruments, has undergone limited radiation-testing (ref 3). For this device the dose-rate effects (induced noise and photocurrent) were about an order of magnitude less than that in the HP 5082-4201 photodetectors; in the total-dose and particle flux environments <5 percent gain degradation and shifts in quiescent operating voltages and currents have occurred.

CONNECTORS AND COUPLERS

Connectors and couplers join various components in fiber optic systems. In all cases, this joining is from a fiber to another component (which may also be a fiber). Generally, the connections are made simply by butting the components. Lensing and other focusing schemes may be used, but they make alignment much more critical. As a result, most of the connectors are mechanical alignment devices, although index-matching fluids are sometimes used to decrease loss.

With a short optical path in the index-matching fluid, the radiation-induced absorption coefficient or luminescence would have to be extremely high to displace radiation effects in the fibers. Furthermore, it is unlikely that radiation would affect the mechanical properties of the connector before it would affect the semiconductor devices. Therefore, connectors can be considered to be unaffected by radiation.

Couplers are more complicated than connectors since they must divide or mix the light as well as mechanically join the components. Usually they make use of a short length of optically transparent material, which would likely be one from which fibers are made.

Degradation Level	Specific Effect	Coupler
Transient Ionization Effects	Transient upset signal	10^{6} - 10^{9} rd(Si)/s
	Transient signal loss (immediate)	10^{11} - 10^{12} rd(Si)/s
	Transient signal loss (1 ms)	10^{11} - 10^{12} rd(Si)/s
	Transient signal loss (1 s)	10^{11} - 10^{14} rd(Si)/s
Permanent Degradation	Ionization-induced signal loss	10^{5} - 10^{8} rd(Si)/s
Thermomechanical Effects	Mechanical failure	10 cal/g(Au)

Table 13. Damage threshold of couplers

Radiation could affect couplers by producing absorption or luminescence in the optical material. Because of the relatively short length of a coupler compared to a fiber, it is more likely that the fiber would set the system vulnerability level. However, couplers which must be radiation-tolerant must not be constructed of radiation-soft glass or other radiation-soft material, since they are long enough that the additional absorption produced by radiation would adversely affect system hardness. Most couplers currently being built have not been designed with radiation hardness in mind; therefore, it is possible that some would not have sufficient hardness. Although experimental test data are not available, it is probably not necessary to radiation-test these components, but merely to exercise reasonable material choice in their design and construction. Choice of the proper materials can be made using the information available from fiber tests, unless some entirely new material (other than glass or plastic) is used.

Thresholds were estimated from this information, and the results are listed in table 13. Coupler length of 2 cm was assumed. Radiation-soft couplers are assumed to be made from doped-silicate glass or doped silica, and radiation-hard couplers are assumed to be made from the appropriate glass or plastic material.

SYSTEM TRADEOFF CONSIDERATIONS

INTRODUCTION

In earlier sections of this report, the radiation vulnerabilities of fiber optic components were presented. This section considers the system design tradeoffs necessary to maintain system performance during and/or after exposure to a radiation environment when the above mentioned components are used. For purposes of this discussion, the system considered will consist of general-purpose black boxes which transmit information via fiber

optic cables. The communication system, whether it is analog or digital, is designed to transfer information at some rate from one black box to another. A consideration for the system designer is whether the disruption of the information transfer can be tolerated, and, if so, how long it may exist before becoming detrimental to the system. Once these questions are answered, the designer should determine which of the component vulnerabilities will produce disruption of the information transfer. The vulnerabilities should then be categorized as to whether they produce (1) catastrophic failures, (2) permanent degradation, or (3) transient upsets in the system, as discussed in previous sections.

CATASTROPHIC FAILURES

For components having vulnerabilities which will produce catastrophic failures, radiation protection must be incorporated into the design. Various methods of providing radiation protection are available and are similar to those required for hardening of electronic circuits. These include shielding, circumvention, EMP protection, photocurrent compensation and/or limiting.

Light Sources

As discussed previously, burnout of light sources is possible at some system threat levels, and shielding may be a solution to this problem. This is possible because the mounting for these components provides two functions heat sinking and optical alignment. With proper design and choice of materials for the mountings, they may provide radiation shielding. However, to provide enough shielding to reduce the threat level to below that which will produce catastrophic failures may result in size and weight increases. The choice of materials is critical because they must provide attenuation of the radiation and good thermal conductivity.

Additional hardening may be added at the circuit level by limiting the maximum current flow through the device to below that which will produce an instantaneous power dissipation that would be required to reach the burnout threshold. This may be accomplished by inserting a resistor in series with the light source. However, this resistor and the device junction capacitance will now provide an RC rolloff which may be below the system's required bandwidth. To compensate for the rolloff, the resistor may be bypassed by a capacitor, the size of which must be limited to a value that will not store enough energy to cause burnout in the light source.

For circuits in which the above current-limiting technique cannot be employed because of system constraints such as bandwidth, circumvention may be used to interrupt the power source at the circuits. This will result in a loss of data transfer during the circumvention period, but will prevent burnout of the light source and its drive circuitry.

Light Detectors

For the purposes of this discussion, it is assumed that the types of semiconductor light detectors most likely to be used in military systems are the pin and avalanche photodiodes. These devices are similar in circuit operation in that they both are reverse-biased into depletion. Because they are light detectors they also respond to incident ionizing radiation; therefore, photocurrent protection is essential. Here again, because these devices are usually mounted in connectors that provide optical alignment with the fibers, it is possible to select materials for their construction that will provide radiation shielding. The obvious weight and size tradeoffs are the governing factors.

Since photocurrent generation in a device is directly proportional to the volume of the active region in the detector, it is beneficial to reduce the volume as much as possible. This would indicate that detectors having the smallest active area should be used in critical systems. However, the design tradeoff here is that of collecting enough light signal exiting the fiber optic cable. Since the light exits the cable at its numerical aperture, the design should place the end of the fiber optic cable as close as possible to the detector.

Also, reduction of the area of the junction implies that the burnout threshold is lower (ref 11,12). It is then necessary to maximize the area/volume ratio. To limit the current flow through the detector to prevent burnout, a resistor may be added between the bias supply and the detector; however, this resistor now would produce an additional noise source at the input to the amplifier. It should, therefore, be bypassed by a capacitor whose size must be limited.

Circumvention may also be considered for the light detector bias circuitry to provide radiation protection. But because the bias supply may be a relatively high voltage supply (>50V) derived from a lower one (ie, a dc-to-dc converter), the time required to return to the designed detector bias voltage would be greater than the circumvention time; thus, signal outage time may be increased. Some state-of-the-art pin diodes may be operated from the 5-V logic supply bus, which makes circumvention very practical for these devices.

PERMANENT DEGRADATION

Some of the radiation damage produced within the fiber optic components results in permanent degradation. Some effects may be annealed out by baking the components at elevated temperatures for relatively long time periods (minutes to hours to days), but at normal operating temperatures the parameter degradation may be considered permanent. Parameter degradations may result in a decrease in the electro-optical conversion efficiencies of semiconductor components or in increased attenuation coefficients for fiber optic cables, causing a decrease in the quality of information transfer between the fiber optics system black boxes.

Light Sources

The major concern for the designer when using semiconductor light sources in radiation environments is how to compensate for the decrease in light power output of these devices. One method is to use brute force and increase the operating current through them to allow for the decrease in optical power output. Although this will solve the power problem, the method has shortcomings; it decreases the operating lifetime of the source. Therefore, when the designer uses this method he must consider this consequence as well as the increased electrical power and heat-sinking requirements.

Another method is to use an active feedback circuit to adjust the drive current through the source. This method has the feature of not increasing the current through the device until degradation has occurred. It has the disadvantage that an optical detector must be placed in such a position that it samples the light output of the source. It is for this reason that the method is usually applied only to edge-emitter sources so that the detector and its amplifier circuitry may be placed behind the chip in the same package. This increases the cost of the source and the complexity of the light source drive circuitry.

A unique problem exists when using laser diodes in a radiation environment; the threshold current (the minimum current at which lasing action will begin) will increase with increasing radiation. This will result in two detrimental effects on the system – reduction of dynamic range and slower turn-on. For analog systems in which the signal's dynamic range is important, the maximum signal swing is limited by the difference between the quiescent current-biasing point and the threshold current. Therefore, when the threshold current increases, signal distortion will occur at lower signal levels. For those systems in which the high-frequency response of the laser diode is important, the quiescent operating current is selected to be just above the threshold current level, to minimize the turn-on time. If the threshold current increases above that of the quiescent current due to radiation exposure, a decrease in the high-frequency response is inevitable. If the designer tries to compensate for this shift by increasing the quiescent bias current, he must consider that the on-to-off light power level ratio will be reduced, and that the power dissipation in the laser diode will increase and will result in a shorter operating lifetime.

Cables

To compensate for the increase in fiber absorption caused by radiation, the designer has four areas in which he may work. The first is the choice of materials from which the fiber optic cable is manufactured, as discussed earlier, along with their relative radiation responses and optical properties. Second, the relative power output of the light source may be increased to provide an adequate design margin after radiation. The third method is to provide radiation shielding, which may not be a solution for some systems because of cable size and weight increases. Finally, the system architecture may be designed to allow for system outage times.

The major concerns for the designer when using semiconductor photodetectors in radiation environments are dark current increases and reduced device gain, or conversion efficiency and noise generation.

Dark current increases are particularly bothersome to systems in which dc signal response is required because this current is summed with the signal current at the detector amplifier output. Under normal design practices, this current is at least an order of magnitude below the minimum detectable light signal; however, it is possible that, at some system threat levels, the dark current could increase by two to three orders of magnitude. This could easily cause a dc-responding amplifier to be forced out of the linear region into saturation, resulting in loss of signal. Since this current originates in the surface areas and depletion regions of the semiconductor junctions, it would be beneficial to select devices that have small active areas, as discussed earlier. To compensate for the increase in current into the summing point at the amplifier input, a matched diode that is not exposed to the input optical signal may be added to provide an alternate current path around the summing point.

In systems in which adequate S/N ratios exist automatic gain control (AGC) may be designed into the photodetector amplifier to compensate for the reduced gain or conversion efficiency in the detector. This will result in an increase in the complexity of the amplifier design and in the analysis of amplifier response to transient radiation exposure.

Shielding may also be employed to provide radiation hardening to protect the detector from dark-current increases.

TRANSIENT EFFECTS

Transient radiation effects on the fiber optic components produce an addition of false signals into the data and/or temporary loss of signal. The designer must determine if these effects will produce detrimental system response, and design against them if they cannot be tolerated.

Light Sources

In systems in which data transmission is required during the radiation pulse, particular care must be taken to compensate for photocurrents generated within the source's modulating circuitry. The photocurrents must be limited to a level that will result in a current through the source that will produce a minimum detectable optical signal from the source. This may require matching photocurrent responses in devices, which becomes a very difficult procurement problem, or providing radiation shielding to the entire modulating circuitry.

For systems in which data interruption may occur but no false signals may be produced, circumvention is a possibility. As long as the system does not accept information during this time, it does not matter if the source is momentarily turned on or off.

Cables

Transient ionization effects in fiber optic cables produce two phenomena that are of concern to the designer - luminescence and increase in attenuation. Their mechanisms and their effects on the system were discussed earlier. This section concerns system design alternatives that may be used to reduce or eliminate the unwanted responses from the system.

The luminescence problem exists in only those systems that require data transmission during the radiation, and may be reduced by adding optical bandpass filters between the end of the cable and the photodetector. This will result in increased attenuation of optical signals outside the transmitted bandwidth, with little attenuation of the data signal. Care should be taken when selecting materials from which to construct the filters to choose materials that will not luminesce. Adding the filters at the detector will increase the complexity of the connector design and will necessarily increase the distance between the end of the fiber optic cable and the detector. This will result in further spreading of the exiting light, which may require a larger-area detector or lensing to collect all the available light signal. If pigtailed detectors are used, the filters have to be added at the connector that mates the end of the pigtail with the end of the fiber. This will increase the connector losses for most connectors significantly, and will virtually eliminate all low-loss connectors (<1 dB).

Transient absorption increases in fiber optic cables present a problem to the designer because they can require relatively long periods in which to recover, resulting in significant periods of signal outage which some systems cannot tolerate. This problem can be counteracted by increasing the power output of the light source and, for systems with large S/N ratios, using AGC circuits in the photodetector amplifier circuitry. The consequences of both these actions have been discussed previously. The reduction in outage time may not be significant for large induced transient absorption (much greater than the design margin). With some of the newer fiber optic cables this problem has been greatly reduced and the choice of one of these cables may eliminate the problem. For ground-based systems, the cables may be buried in the earth to provide the required shielding.

Detectors

For systems that must operate through transient radiation exposures, a significant problem exists with the photodetectors. The photocurrents generated within the detectors may be several orders of magnitude larger than the optical signals; therefore, some method of preventing these currents from entering the detector amplifier circuitry must be found. One design solution is to use radiation shielding to protect the detector, the consequences of which have been discussed earlier. Another method is to add another matched diode that is not exposed to the input optical signal and which will provide an equal but opposite photocurrent out of the summing point. The added diode should not be confused with the "guard-ring" diode contained in some detectors. Adding this diode may create a problem in systems in which small S/N ratios are anticipated, since its noise will add to the noise of the optical detector and reduce the S/N ratio by 3 dB.

Exposure of the photodetector to steady-state ionizing radiation will produce a noise signal that will degrade the system S/N ratio. To provide rejection of out-of-band noise, the designer should limit the bandpass of the detector amplifier circuitry to the minimum required for data transfer. This will complicate the circuit design of the amplifier and may put additional constraints on its open-loop gain and frequency response. In systems in which large bandwidths are required, it will be necessary to provide shielding for the photodetector or to increase the optical signal level at the input to the detector. Earlierdiscussions describe the consequences of both these actions.

SUMMARY EVALUATION OF THE APPLICABILITY OF FIBER OPTICS TO GENERIC MILITARY SYSTEMS

The vulnerabilities of fiber optic systems are compared to environment levels for various system types. For all levels, 120 dB attenuation of the free-field EMP is assumed. These generic examples provide gross guidelines for applicability to military systems.

RE-ENTRY VEHICLE SYSTEMS

For cables installed inside the heat shield but outside the electronic component X-ray shield the ionization dose delivered to a fiber optic cable is such that none of the systems discussed in this report will recover operation within 10 minutes of exposure. Even for the doses assumed to be within the X-ray shield, the links will require 1 second or longer to recover to operability. No fiber optic system examined in this report appears to be readily applicable to a re-entry vehicle system.

SATELLITE SYSTEMS

EMP fields are of relatively small magnitude for satellites, thus satellite data links are not expected to be significantly vulnerable. For satellites hardened to JCS levels, fiber optic systems have limited applicability, and then only if shielding is provided. The amount of shielding required is such that there is no advantage over a hard-wired link from a radiation effects point of view. Fiber optic systems are applicable to hardened satellites at levels near 10^{-3} JCS, and on unhardened satellites provided the photodetector is adequately protected against noise from electrons in the belt. The amount of protection required is orbit and scenario-specific.

STRATEGIC SYSTEMS

The large prompt dose absorbed by strategic missile components when exposed to the in-flight radiation environment makes all the fiber optic systems considered here inapplicable without considerable shielding. The amount of shielding is such that fiber optic systems have no advantage in weight or size compared to a hard-wired link.

None of the links will operate through the example environment without further shielding. The links will recover from both the flight threat example and the ground example in 10 ms or less. For an aircraft which may be exposed to the EMP threat without the direct radiation environment, only the 1, 10, and 100-Mbit point-to-point links will meet the operate-through requirement attenuated by 120 dB for the EMP threat.

For ground facilities, all the fiber optic systems considered here will recover from exposure to the example threat within 1 ms of exposure if the entire system is protected by two metres or more of earth. Because of the EMP environment, the operate-through requirement can be met for less than 100 m of cable by burial of the electronics at a depth of five metres or greater.

In the 1 to 10-ms time regime, the delayed components of the radiation environment cause inoperability of the link. For scenarios for which there is negligible (less than 10^{-3} rd) ionizing radiation deposited in aircraft components, the 1, 10, and 100-Mbit point-to-point lengths will operate through exposure of the aircraft to the EMP threat, assuming 120 dB attenuation of the free-field threat at the component level. It is anticipated that the other types of links will upset but will return to operation after a few hundred nanoseconds

of upset by the EMP pulse. It is for those scenarios in which the TRE environment has been reduced, either by distance or by shielding, that firm conclusions about the applicability of a fiber optic data link to a specific aircraft system must be based on an understanding of the details of the system geometry and shielding. The EMP environment at the susceptible component can easily vary over several orders of magnitude for slight changes in the electronic enclosure configuration or power supply line shielding. Hence, general conclusions about the applicability of fiber optics to aircraft systems where the TRE levels have been reduced cannot be made.

TACTICAL SYSTEMS

The range of tactical scenarios is such that it is impossible to summarize in a brief document the applicability of fiber optic systems to a generic tactical situation. However as an example, none of the links will meet an operate-through requirement even 10 km from a 1-kt surface burst. All the links will recover 1 ms after exposure to a 1-kt surface burst at a 0.5-km slant range. At the 8-psi level (0.03 km from a 1-kt surface burst), only the 100-m, 1-Mbit link will recover in 1 ms. The remaining links require 10 seconds or longer to recover. Fiber optic data links could be considered functional in tactical situations, but the degree depends upon both the application and the anticipated scenario.

RECOMMENDATIONS.

It is recommended that fiber optics be considered in the design of any system whose cable runs are greater than ten metres and which must adhere to military system EMP requirements.

It is recommended that fiber optics be considered in the design of any system whose recovery times are greater than millisecond, and whose dose rate and total dose deliverance are within the budget link design margin.

It is also recommended that fiber optics be considered in the design of any system whose operation is dependent upon the survivability of its personnel, where personnel nuclear survivability requirements are the limiting factor in the system's operation.

Additional data must be obtained to ascertain the displacement damage-producing effects on fiber optic systems.

REFERENCES

1. Vance, EF, Coupling to Shielded Cables, Wiley-Interscience, 1978
2. AFAL TR-45, Opto-electronics Aspects of Avionic System II, by JR Baird, May 1975
3. Hardwick, WH, and Kalma, AH, Effects of low-Dose-Rate Radiation on Opto-Electronic Components and the Consequences on Fiber Optic Data Link Performance, IEEE Trans Nucl Sci NS-26, No 6, December 1979
4. ERADCOM TR-28-13, Nuclear Radiation Vulnerability of Proposed Army Fiber Optics Communications System, by S Kronenberg, et al, 1978
5. Arimura, I, and Colwell, R, Radiation Degradation and Recovery in Long Fiber Optic Data Links, presented at 1978 Symposium on Fiber Optics in Nuclear Environment, March 25-27, 1980
6. Sigel, GH, Jr, et al, Radiation Response of Large-Core Polymer-Clad Silica Optical Fibers, IEEE Trans Nucl Sci NS-26, No 6, December 1979
7. NOSC Report TR-469, EMP Hardening of Airborne Systems through Electro-optical Techniques: Design Guideline, by R Greenwell, 15 December 1979
8. IRT Report 4521-002, The ABCs of Radiation Hardening, April 1976
9. IRT Final Report for AFWL, Fiber Optic Radiation Test and Evaluation Program, Kirtland AFB, December 1978
10. Motorola Application Note AN-707, Noise Immunity Comparison of CMOS vs Popular Bipolar Logic Families, by AA Allen, 1973
11. Wunsch, DC, and Bell, RR, Determination of Threshold Failure Levels of Semiconductor Diodes and Transistors Due to Pulse Voltage, IEEE Trans Nucl Sci NS-17, 364, 1970
12. Tasca, DN, Pulse Power Failure Modes in Semiconductors, IEEE Trans Nucl Sci NS-17, 364, 1970
13. AFWL TR-74-302, An Assessment of Fiber Optics Technology for Satellite Hardening, by AH Kalma, 1975
14. Kalma, AH, and Fisher, CJ, Electrical Pulse Burnout Testing of Light-Emitting Diodes, IEEE Trans Nucl Sci NS-22, 2510, 1975
15. O.Brien, JT, et al, Recent Developments in Injection Lasers, presented at Conference on Laser and Electro-Optical Systems, San Diego, California, 25-27 May, 1976
16. AFWL TR-68-31, vol 2, Radiation Effects on GaAs Devices and Schottky Diodes, by HD Southward and RH Schnurr, August 1968
17. Northrop Report DN A3776F, Study of Radiation Effects in Bulk CMOS Microcircuits, IIL/LSI Logic Cells, and Optic Couplers, by JP Raymond, et al, 1975

18. Barnes, CE, Development of Efficient Radiation-Insensitive GaA:Zn LEDs, IEEE Trans Nucl Sci NS-24, No. 6, December 1977

19. AFAL TR-74-61 Survey of Vulnerability of Contemporary Semiconductor Components to Nuclear Radiation, by RP Donovan, et al, 1974

20. Epstein, AS, et al, Gamma Irradiation and Annealing Effects in Nitrogen-Doped GaAsP Green and Yellow Light-Emitting Diodes, IEEE Trans Nucl Sci NS-19, 386, 1972

21. Barnes, CE, Effects of ^{60}Co Gamma Irradiation on Epitaxial GaAs Laser Diodes, Phys Rev B1, 4735, 1970

22. Schnurr, RH, and Southward, HD, Radiation Effects on GaAs Devices, IEEE Trans Nucl Sci NS-15, 306, 1968

23. Soda, KJ, et al, The Effect of Gamma Irradiation on Optical Isolators, IEEE Trans Nucl Sci NS-22, 2475, 1975

24. Polimadei, RA, et al, Performance of GaAlAs Light-Emitting Diodes in Radiation Environments, IEEE Trans Nucl Sci NS-21, 96, 1974

25. Share, S, et al, Radiation Effects and Hardening on Compensated GaAs Light-Emitting Diodes, IEEE Trans Nucl Sci NS-20, 256, 1973

26. Epstein, AS, et al, Radiation Effects on Active and Passive Optical Components, presented at DoD/Industry-Wide Integrated Optics and Fiber Optics Communications Conference, NELC, San Diego, California, 1974

27. Schroeder, JD, et al, *Radiation-Damage-Induced Time Delay in GaAs Lasers*, IEEE Trans Nucl Sci NS-19, 391, 1972

28. Epstein, AS, and Trimmer, PA, Radiation Damage and Annealing Effects on Photon-Coupled Isolators, IEEE Trans Nucl Sci NS-19, 391, 1972

29. Barnes, CE, Radiation Effects in Electroluminescent Diodes, IEEE Trans Nucl Sci NS-18, 322, 1971

30. Noel, BW, et al, Neutron Irradiation Effects on Diffused GaAs Laser Diodes, IEEE Trans Nucl Sci NS-18, 378, 1971

31. Barnes, CE, Neutron Damage in Epitaxial GaAs Laser Diodes, J Appl Phys 42, 1941, 1971

32. Schade, H, et al, Defect Centers in GaAsP Electroluminescent Diodes Due to High-Energy Electron Irradiation, J Appl Phys 41, 3783, 1970

33. Barnes, CE, Neutron Damage in GaAs Laser Diodes at and above Laser Threshold, IEEE Trans Nucl Sci NS-19, 382, 1972

34. Epstein, AS, et al, Effect of Neutron Irradiation on GaAsP Electroluminescent Diodes, Appl Phys Lett 23, 472, 1973

35. Stanley, AG, Comparison of Light-Emitting Diodes in a Space Radiation Environment, IEEE Trans Nucl Sci NS-17, 239, 1970

36. Sandia Report SC-RR-710686 Radiation Effects in Light-Emitting Diodes and Laser Diodes, by CE Barnes, 1972

37. Barnes, CE, Neutron Damage in GaP Light-Emitting Diodes, Appl Phys Lett 20, 110, 1972

38. Compton, DMJ, and Cesena, RA, Michanism of Radiation Effects on Lasers, IEEE Trans Nucl Sci NS-14, 55, 1967

39. Arnold, GW, Luminescence in Intrinsic and Annealed Electron-Irradiated GaAs:Cd, Phys Rev 183, 777, 1969

40. Barnes, CE, Appl Phys Lett 20, 86, 1972

41. Barnes, CE, Tunneling in SiC Electroluminescent Diodes, J Appl Phys 45, 193, 1974

42. Barnes, CE, Increased Radiation Hardness of GaAs Laser Diodes at High Current Densities, J Appl Phys 45, 3485, 1974

43. Evans, BD, and Sigel, GH, Jr, Radiation-Resistant Fiber Optic Materials and Waveguides, IEEE Trans Nucl Sci NS-22, 2462, 1975

44. Mattern, PL, et al, Effects of Radiation on Absorption and Luminescence of Fiber Optic Waveguides and Materials, IEEE Trans Nucl Sci NS-21, 81, 1974

45. Evans, BD, and Sigel, GH, Jr, Permanent and Transient Radiation-Induced Losses in Optical Fibers, IEEE Trans Nucl Sci NS-21, 113, 1974

46. NRL Memorandum Report 2704, Radiation Effects in Fiber Optic Waveguides, by GH Sigel, Jr, 1973

47. Mattern, PL, Radiation-Induced Absorption and Luminescence in Glass and Plastic Optical Waveguides, presented at DoD/Industry-Wide Integrated Optics and Fiber Optics Communications Conference, NELC, San Diego, California, 1974

48. NRL Memorandum Report 2934, Radiation Effects in Fiber Optic Waveguides, by GH Sigel, Jr, et al, 1974

49. AFCRL TR-74-0012, Transient Radiation Effects Tests of a Corning Radiation-Resistant Optical Fiber, by JA Wall, 1975

50. AFCRL TR-75-0190, Radiation Effects on Fiber Optics, by JA Wall and JF Bryant, 1975

51. Mattern, PL, et al, Effects of Radiation on Optical Fibers and Materials, IEEE Trans Nucl Sci NS-22, 2468, 1975

52. Sandia Report SAND76-8056, A Summary of Radiation-Induced Transient Absorption and Recovery in Fiber Optic Waveguides, by CD Skoog, 1976

53. IRT Report INTEL RT 8111-089, Fiber Optics Test Program for Satellite Applications, by AH Kalma and WH Hardwick

54. Kalma, AH, and Hardwick, WH, Radiation Testing of a Fiber Optics Data Link, IEEE Trans Nucl Sci NS-23, 1769, 1976

55. Maurer, RD, et al, Effects of Neutron and Gamma Radiation on Glass Optical Waveguides, Appl Opt 12, 2024, 1973

56. Sigel, GH, Jr, and Evans, BD, Effects of Ionizing Radiation on Transmission of Optical Fibers, Appl Phys Lett 24, 410, 1974

57. Acharekar, MA, Multimode Radiation-Resistant Glass Fiber for Data Transmission Applications, presented at Dod/Industry-Wide Integrated Optics and Fiber Optics Communications Conference, NELC, San Diego, California, 1974

58. Sigel, GH, Jr, Radiation Damage in Fiber Optics, presented at DoD/Industry-Wide Integrated Optics and Fiber Optics Communications Conference, NELC, San Diego, California, 1974

59. Friebele, EJ, et al, Radiation Protection of Fiber Optics Materials: Effects of Oxidation and Reduction, Appl Phys Lett 24, 412, 1974

60. Friebele, EJ, et al, Defect Centers in a Germanium-Doped Silica-Core Optical Fiber, J Appl Phys 45, 3424, 1974

61. Baba, A, et al, Effect of Simulated Nuclear Thermal Pulses on Fiber Optic Cables, IEEE Trans Nucl Sci NS-26, No 6, December 1979

62. Radiation Testing of Photodetectors, Final Report, Contract F29601-76-C-0034, by WH Hardwick and AH Kalma, February 1978

63. DNA 1420H-1 TREE Handbook, vol 1, by RK Thatcher, 1971

64. HDL DS-94-1, Radiation Effects on Semiconductor Devices Summary Report, Components Response Information Center (DNA Data Bank), June 1974

65. Gulf RT C12375, Status of Integrated Circuits, by LD Cotter and MA Donaldson, November 1975

66. Gwyn, CW, Analysis of Radiation Effects in Semiconductor Junction Devices, IEEE Trans Nucl Sci NS-14, No 6, December 1967

67. IRT Report INTEL RT 0040-001, by AH Kalma, August 1976

68. IRT Report INTEL RT 0039-001, Irradiation Testing of Optics Components, by AH Kalma and RA Cesena

69. Brucker, GJ, and Cope, AD, Radiation Sensitivity of Silicon Imaging Sensors on Missions to the Outer Planets, IEEE Trans Nucl Sci NS-19, 147, 1972

70. Jet Propulsion Laboratory Report 21945-6001-RV-00, Solar Cell Radiation Handbook, by JR Carter, Jr, and HY Tada, June 1973

INITIAL DISTRIBUTION

DEPARTMENT OF DEFENSE

DIRECTOR
ARMED FORCES RADIOBIOLOGY RESEARCH INSTITUTE
DEFENSE NUCLEAR AGENCY
NATIONAL NAVAL MEDICAL CENTER
BETHESDA, MD 20014
ATTN: ADLF

ASSISTANT TO THE SECRETARY OF DEFENSE
ATOMIC ENERGY
WASHINGTON, DC 20301
ATTN: EXECUTIVE ASSISTANT

DIRECTOR
DEFENSE ADVANCED RESEARCH PROJECTS AGENCY
100 WILSON BLVD.
ARLINGTON, VA 22209
ATTN: T10

DIRECTOR
DEFENSE CIVIL PREPAREDNESS AGENCY
WASHINGTON, DC 20301
ATTN: PLANS & OPERATIONS (EO)
ATTN: PLANS & OPERATIONS (SE)

DIRECTOR
DEFENSE COMMUNICATIONS AGENCY
WASHINGTON, DC 20305
ATTN: CODE C313

DEFENSE COMMUNICATIONS ENGINEERING CENTER
1860 WIEHLE AVENUE
RESTON, VA 22090
ATTN: CODE R400
ATTN: CODE R720 (C. STANSBERRY)
ATTN: CODE R123 (TECH LIB)

DEFENSE DOCUMENTATION CENTER
CAMERON STATION
ALEXANDRIA, VA 22314
ATTN: DD (12)

DIRECTOR
DEFENSE INTELLIGENCE AGENCY
WASHINGTON, DC 20301
ATTN: RDS-3A (TECH LIB)
ATTN: DB-4C (E. O'FARRELL)

DIRECTOR
DEFENSE NUCLEAR AGENCY
WASHINGTON, DC 20305
ATTN: RATN
ATTN: STVL
ATTN: DDST
ATTN: RAEV
ATTN: TITL (4)

COMMANDER
FIELD COMMAND
DEFENSE NUCLEAR AGENCY
KIRTLAND AFB, NM 87115
ATTN: FCLMC

CHIEF
FIELD COMMAND
DEFENSE NUCLEAR AGENCY
LIVERMORE DIVISION
P.O. BOX 808 L-317
LIVERMORE, CA 94550
ATTN: FCPRL

DIRECTOR
INTERSERVICE NUCLEAR WEAPONS SCHOOL
KIRTLAND AFB, NM 87115
TTV

JOINT CHIEFS OF STAFF
WASHINGTON, DC 20301
ATTN: J-3

DIRECTOR
JOINT STRAT TGT PLANNING STAFF
OFFUTT AFB
OMAHA, NE 68113
ATTN: JLTW-2
ATTN: NRI-STINFC LIBRARY

NATIONAL COMMUNICATIONS SYSTEM
OFFICE OF THE MANAGER
DEPARTMENT OF DEFENSE
WASHINGTON, DC 20305
ATTN: NCS-TS (D. BODSON)

DIRECTOR
NATIONAL SECURITY AGENCY
FORT GEORGE G. MEADE, MD 20755
ATTN: S-232 (C. VINCENT)
ATTN: TCL
ATTN: R-52 (C. VAN GUNTEN)

UNDER SECRETARY OF DEFENSE FOR RESEARCH & ENGINEERING
DEPARTMENT OF DEFENSE
WASHINGTON, DC 20301
ATTN: STRATEGIC & SPACE SYSTEMS (OS)

DEPARTMENT OF THE NAVY

COMMANDER
NAVAL AIR SYSTEMS COMMAND
WASHINGTON, DC 20361
ATTN: AIR-350F
ATTN: AIR-360
ATTN: PMA-257
ATTN: PMA-231
ATTN: PMA-234
ATTN: PMA-265
ATTN: PMA-240

OFFICER IN CHARGE
NAVAL CONSTRUCTION BATTALION CENTER
CIVIL ENGINEERING LABORATORY
PORT HUENEME, CA 93041
ATTN: CODE L08A (LIBRARY)

COMMANDER
NAVAL ELECTRONIC SYSTEMS COMMAND
WASHINGTON, DC 2-360
ATTN: PME 117-21

COMMANDING OFFICER
NAVAL INTELLIGENCE SUPPORT CENTER
4301 SUITLAND ROAD, BLDG. 5
WASHINGTON, DC 20390
ATTN: CODE 41

COMMANDER
NAVAL OCEAN SYSTEMS CENTER
SAN DIEGO, CA 92152
ATTN: CODE 7309 (R. GREENWELL) (30)
ATTN: CODE 8123 (S. LICHTMAN)
ATTN: CODE 8251 (R. KOCHANSKI)
ATTN: CODE 8105 (J. ROCKWAY)
ATTN: CODE 9241 (E. SCHAEFER)

COMMANDING OFFICER
NAVAL ORDNANCE STATION
INDIAN HEAD, MD 20640
ATTN: STANDARDIZATION DIVISION

SUPERINTENDENT
NAVAL POSTGRADUATE SCHOOL
MONTEREY, CA 93940
ATTN: CODE 1424 (LIBRARY)

COMMANDING OFFICER
NAVAL RESEARCH LABORATORY
WASHINGTON, DC 20375
ATTN: CODE 1434 (E. BRANCATO)
ATTN: CODE 6624
ATTN: CODE 2627 (D. FOLEN)

COMMANDER
NAVAL SEA SYSTEMS COMMAND
WASHINGTON, DC 20362
ATTN: NSEA-61433 (E. DUFFY)

OFFICER IN CHARGE
NAVAL SURFACE WEAPONS CENTER
WHITE OAK LABORATORY
SILVER SPRING, MD 20910
ATTN: CODE R43 (L. LIBELO)
ATTN: CODE F30
ATTN: CODE F32 (E. RATHBUN)

COMMANDER
NAVAL SURFACE WEAPONS CENTER
DAHLGREN, VA 22448
ATTN: CODE F-56

COMMANDER
NAVAL WEAPONS CENTER
CHINA LAKE, CA 93555
ATTN: CODE 233 (TECH LIB)

COMMANDING OFFICER
NAVAL WEAPONS EVALUATION FACILITY
KIRTLAND AFB
ALBUQUERQUE, NM 87117
ATTN: CODE AT-6

CHIEF OF NAVAL OPERATIONS
NAVY DEPARTMENT
WASHINGTON, DC 20350
ATTN: NOP-981
ATTN: NOP-981N1

DIRECTOR
STRATEGIC SYSTEMS PROJECT OFFICE (PM-1)
DEPARTMENT OF THE NAVY
WASHINGTON, DC 20376
ATTN: NSP-230 (D. GOLD)
ATTN: NSP-2342 (R. COLEMAN)
ATTN: NSP-2701 (J. FITSENBERGER)
ATTN: NSP-43 (TECH LIB)
ATTN: NSP-27334

DEPARTMENT OF THE ARMY

DIRECTOR
BMD ADVANCED TECHNOLOGY CENTER
DEPARTMENT OF THE ARMY
P.O. BOX 1500
HUNTSVILLE, AL 35807
ATTN: ATC-T (11)

COMMANDER
BMD SYSTEMS COMMAND
DEPARTMENT OF THE ARMY
P.O. BOX 1500
HUNSTVILLE, AL 35807
ATTN: BMDSC-ACLIB

DEPUTY CHIEF OF STAFF FOR RESEARCH AND ACQUISITION
DEPARTMENT OF THE ARMY
WASHINGTON, DC 20310
ATTN: DAMA-CSS-N (N. BARRON)

COMMANDER
ELECTRONICS TECHNOLOGY AND DEVICES LABORATORY
U.S. ARMY ELECTRONICS R&D COMMAND
FORT MONMOUTH, NJ 07703
ATTN: DELSD-L (W. WERK)
ATTN: DELCS-K (A. COHEN)
ATTN: DELET-IR (E. HUNTER)
ATTN: DRDCO-CCM-ME (G. GAULE)

COMMANDER
HARRY DIAMOND LABORATORIES
DEPARTMENT OF THE ARMY
2800 POWDER MILL ROAD
ADELPHI, MD 20783
ATTN: DELHD-RBH
ATTN: DELHD-N-EMD
ATTN: DELHD-NRBA
ATTN: DELHD-N-P
ATTN: DELHD-I-TL (TECH LIB)
ATTN: DELHD-N-EM (CHIEF EME LAB)
ATTN: DELHD-N-TF
ATTN: DELHD-N-TD
ATTN: DELHD-N-EMA
ATTN: DELHD-N-RCC
ATTN: DELHD-N-EM-C
ATTN: DELHD-N-EMB
ATTN: DELHD-N-EME
ATTN: DELHD-N-RB

PROJECT MANAGER
MULTI-SERVICE COMMUNICATIONS SYSTEMS
DEPARTMENT OF THE ARMY
FORT MONMOUTH, NJ 07703
ATTN: DRCPM-MSCS-APB (M. FRANCIS)

COMMANDER
U.S. ARMY ARMOR CENTER
FORT KNOX, KY 40121
ATTN: TECHNICAL LIBRARY

U.S. ARMY AVIATION RESEARCH AND DEVELOPMENT COMMAND
FORT EUSTIS, VA 23604
ATTN: ATL, LT L. O. SMITH

DIRECTOR
U.S. ARMY BALLISTIC RESEARCH LABS
ABERDEEN PROVING GROUND, MD 21005
ATTN: DRDAR-BLE
ATTN: DRDAR-BLV

COMMANDER
U.S. ARMY COMMUNICATIONS-ELECTRONICS ENGINEERING INSTALLATION AGENCY
FORT HUACHUCA, AZ 85613
ATTN: CCC-CED-SES

COMMANDER
U.S. ARMY COMMUNICATIONS COMMAND
FORT HUACHUCA, AZ 85613
ATTN: CC-ENGR
ATTN: ATSI-CD-MD
ATTN: CC-CPS-OS
ATTN: CC-CPS-PD
ATTN: CC-CC-SAP

CHIEF
U.S. ARMY COMMUNICATIONS SYSTEMS AGENCY
FORT MONMOUTH, NJ 07703
ATTN: CCM-RD-T CCM-AD-SV

PROJECT OFFICER
U.S. ARMY ELECTRONICS RESEARCH AND DEVELOPMENT COMMAND
FORT MONMOUTH, NJ 07703
ATTN: DRDCO-SEI
ATTN: DRCPM-ATC

DIVISION ENGINEER
U.S. ARMY ENGINEER DIVISION, HUNTSVILLE
P.O. BOX 1600, WEST STATION
HUNTSVILLE, AL 35807
ATTN: HNDED-SR

U.S. ARMY INTEL THREAT ANALYSIS DETACHMENT
BLDG A, ROOM 2201
ARLINGTON HALL STATION
ARLINGTON, VA 22212
ATTN: ADMIN OFFICER

U.S. ARMY INTELLIGENCE & SEC COMMAND
ARLINGTON HALL STATION
4000 ARLINGTON BLVD.
ARLINGTON, VA 22212
ATTN: TECHNICAL LIBRARY
ATTN: TECH INFO FAC

DIRECTOR
U.S. ARMY MATERIAL SYS ANALYSIS ACTIVITY
ABERDEEN PROVING GROUND, MD 21005
ATTN: DRXSY-PC
ATTN: DRXSY-CC

COMMANDER
U.S. ARMY MISSILE R&D COMMAND
REDSTONE ARSENAL, AL 35809
ATTN: DRCPM-PE-EG (W.. JOHNSON)
ATTN: DRDMI-EAA
ATTN: DRDMI-TBD
ATTN: DRCPM-PE-EA (W. WAGNER)

COMMANDER
U.S. ARMY TEST AND EVALUATION COMMAND
ABERDEEN PROVING GROUND, MD 21005
ATTN: DRSTE-EL
ATTN: DRSTE-FA

COMMANDER
U.S. ARMY TRAINING AND DOCTRINE COMMAND
FORT MONROE, VA 23651
ATTN: ATORI-OP-SW

COMMANDER
WHITE SANDS MISSILE RANGE
DEPARTMENT OF THE ARMY
WHITE SANDS MISSILE RANGE, NM 88002
ATTN: STEWS-TE-AN (J. OKUNA)

DIRECTOR
APPLIED TECHNOLOGY LABORATORY
U.S. ARMY RESEARCH AND TECHNOLOGY LABORATORIES (AURADCOM)
FORT EUSTIS, VA 23604
ATTN: DAVDL-ATL-ASA (LT L. SMITH)

DEPARTMENT OF THE AIR FORCE

COMMANDER
AERONAUTICAL SYSTEMS DIVISION, AFSC
WRIGHT-PATTERSON AFB, OH 45433
ATTN: ASD/ENESH (P. MARTH)
ATTN: ASD/YYEF
ATTN: ASD/ENFTV

COMMANDER
AEROSPACE DEFENSE COMMAND/DE
DEPARTMENT OF THE AIR FORCE
ENT AFB, CO 80912
ATTN: DEE

COMMANDANT
AIR FORCE FLIGHT DYNAMICS LABORATORY
WRIGHT-PATTERSON AFB, OH 45433
ATTN: J. CORBIN

AIR FORCE TECHNICAL APPLICATIONS CENTER
PATRICK AFB, FL 32925
ATTN: TFS M. SCHNEIDER

AIR FORCE WEAPONS LABORATORY, AFSC
KIRTLAND AFB, NM 87117
ATTN: NT
ATTN: EL (C. BAUM)
ATTN: CA
ATTN: ELXT
ATTN: SUL
ATTN: ELT (W. PAGE)
ATTN: NXS
ATTN: ELA (J. CASTILLO)
ATTN: NTN

COMMANDER
AIR LOGISTICS COMMAND
DEPARTMENT OF THE AIR FORCE
HILL AFB, UT 84406
ATTN: OO-ALC/NMETH (P. BERTHEL)
ATTN: OO-ALC/NM (R. BLACKBURN)
ATTN: OO-ALC/NMEDC (L. KIDMAN)

DIRECTOR
AIR UNIVERSITY LIBRARY
DEPARTMENT OF THE AIR FORCE
MAXWELL AFB, AL 36112
ATTN: AUL-LSE-70-250

HEADQUARTERS
ELECTRONIC SYSTEM DIVISION/YS
HANSOM AFB, MA 01731
ATTN: YSEA

COMMANDER
FOREIGN TECHNOLOGY DIVISION
WRIGHT-PATTERSON AFB, OH 45433
ATTN: TCTD (B. BALLARD)
ATTN: NIIS (LIBRARY)

COMMANDER
ROME AIR DEVELOPMENT CENTER, AFSC
GRIFFIS AFB, NY 13441
ATTN: TSLD

COMMANDER
SACRAMENTO AIR LOGISTICS CENTER
DEPARTMENT OF THE AIR FORCE
MCCLELLAN AFB, CA 95652
ATTN: NMCRS (R. DELMASTRO)
ATTN: NMEAE (C. HOWARD)
ATTN: MMCREB

SPACE & MISSILE SYSTEMS ORGANIZATION/IN
AIR FORCE SYSTEMS COMMAND
P.O. BOX 92960
WORLDWAY POSTAL CENTER
LOS ANGELES, CA 90009
ATTN: IND

SPACE & MISSILE SYSTEMS ORGANIZATION/MN
AIR FORCE SYSTEMS COMMAND
NORTON AFB, CA 92409
ATTN: MNNH (M. EARAN)

SPACE & MISSILE SYSTEMS ORGANIZATION/SK
AIR FORCE SYSTEMS COMMAND
P.O. BOX 92960
WORLDWAY POSTAL CENTER
LOS ANGELES, CA 90009
ATTN: SKF

SPACE & MISSLE SYSTEM ORGANIZATION/YA
AIR FORCE SYSTEMS COMMAND
P.O. BOX 92960
WORLDWAY POSTAL CENTER
LOS ANGELES, CA 90009
ATTN YAPC

STRATEGIC AIR COMMAND/XPFS
DEPARTMENT OF THE AIR FORCE
OFFUTT AFB, NB 68113
ATTN: NRI (G. MATZKE)
ATTN: NRI-STINFO LIBRARY
ATTN: XPFS (B. STEPHAN)
ATTN: DEL

COMMANDER
RELIABILITY ANALYSIS CENTER
RADC (RBRAC)
GRIFFISS AFB NY 13441
ATTN: RADC/RBRAC (I. L. KRULAC)

DEPARTMENT OF ENERGY

DEPARTMENT OF ENERGY
ALBUQUERQUE OPERATIONS OFFICE
P.O. BOX 5400
ALBUQUERQUE, NM 87115
ATTN: DOC CON FOR WSSB
ATTN: CTIC

DEPARTMENT OF ENERGY
ECONOMIC REGULATORY ADMINISTRATION
OFFICE OF UTILITIES SYSTEMS
DIV. OF POWER SUPPLY & RELIABILITY (EEPA)
1111 20TH STREET, NW
WASHINGTON, DC 20461
ATTN: OFFICE OF UTILITY SYSTEMS (L. O'NEILL)

OTHER GOVERNMENT (NON DOD)

DIRECTOR
CENTRAL INTELLIGENCE AGENCY
WASHINGTON, DC 20505
ATTN: OSI/NED/NWE

DEPARTMENT OF TRANSPORTATION
FEDERAL AVIATION ADMINISTRATION
HEADQUARTERS, SEC DIV, ASE-300
800 INDEPENDENCE AVENUE, SW
WASHINGTON, DC 20591
ATTN: SEC DIV ASE-300

FEDERAL PREPAREDNESS AGENCY
GENERAL SERVICES ADMINISTRATION
18th & F STREET, NW
WASHINGTON, DC 20405
ATTN: ESTE-M MURTHA

DOD CONTRACTORS

AEROSPACE CORP.
P.O. BOX 92957
LOS ANGELES, CA 90009
ATTN: R. MORTENSEN
ATTN: C. PEARLSTON
ATTN: I. GARFUNKEL
ATTN: LIBRARY
ATTN: C. GREENHOW
ATTN: J. REINHEIMER

AGBABIAN ASSOCIATES
250 N NASH STREET
EL SEGUNDO, CA 90245
ATTN: LIBRARY

AVCO RESEARCH & SYSTEMS GROUP
201 LOWELL STREET
WILMINGTON, MA 01887
ATTN: W. LEPSEVICH

BATTELLE MEMORIAL INSTITUTE
505 KING AVENUE
COLUMBUS, OH 43201
ATTN: E. LEACH

EDM CORP.
7915 JONES BRANCH DRIVE
McLEAN, VA 22102
ATTN: CORPORATE LIBRARY

EDM CORP.
P.O. BOX 9274
ALBUQUERQUE, NM 87119
ATTN: J. SCHWARZ
ATTN: LIBRARY

BENDIX CORP.
COMMUNICATION DIVISION
E JOPPA ROAD
BALTIMORE, MD 21204
ATTN: DOCUMENT CONTROL

BENDIX CORP.
BENDIX CENTER
SOUTHFIELD, MI 48075
ATTN: M. FRANK

BENDIX CORP.
NAVIGATION AND CONTROL GROUP
TETERBORO, NJ 07608
ATTN: DEPT 6401

BOEING CO.
P.O. BOX 3707
SEATTLE, WA 98124
ATTN: C. KEMLE
ATTN: V. JONES
ATTN: H. WICKLEIN
ATTN: KENT TECH LIBRARY
ATTN: B. HANRAHAN
ATTN: D. EGELKROUT

BOEING MILITARY AIRCRAFT CO.
MAIL STOP K75-50
3801 S. OLIVER ST
WICHITA, KS 67210
ATTN: T. HEWLETT
ATTN: L. WELLER

BOOZ-ALLEN AND HAMILTON, INC.
776 SHREWSBURY AVENUE
TINTON FALLS, NJ 07724
ATTN: R. CHRISNER
ATTN: TECH LIBRARY

CALSPAN CORP.
P.O. BOX 400
BUFFALO, NY 14225
ATTN: LIBRARY

CHARLES STARK DRAPER LAB, INC.
555 TECHNOLOGY SQUARE
CAMBRIDGE, MA 02139
ATTN: TIC MS 74
ATTN: K. FERTIG

CINCINNATI ELECTRONICS CORP.
2630 GLENDALE-MILFORD ROAD
CINCINNATI, OH 45241
ATTN: L. HAMMOND
ATTN: C. STUMP

COMPUTER SCIENCES CORP.
6565 ARLINGTON BLVD
FALLS CHURCH, VA 22046
ATTN: R. BRIGGS

COMPUTER SCIENCES CORP.
1400 SAN MATEO BLVD, SE
ALBUQUERQUE, NM 87108
ATTN: A. SCHIFF

CONTROL DATA CORP.
P.O. BOX C
MINNEAPOLIS, MN 55440
ATTN: J. MEEHAN

CUTLER-HAMMER, INC.
AIL DIVISION
COMAC ROAD
DEER PARK, NY 11729
ATTN: E. KARPEN

DIKEWOOD INDUSTRIES, INC.
1009 BRADBURY DRIVE, SE
ALBUQUERQUE, NM 87106
ATTN: L. DAVIS
ATTN: TECH LIBRARY

E-SYSTEMS, INC.
GREENVILLE DIVISION
P.O. BOX 1056
GREENVILLE, TX 75401
ATTN: J. MOORE

EFFECTS TECHNOLOGY, INC.
5383 HOLLISTER AVENUE
SANTA BARBARA, CA 93111
ATTN: S. CLOW

EG&G WASHINGTON ANALYTICAL SERVICES CENTER, INC.
P.O. BOX 10218
ALBUQUERQUE, NM 87114
ATTN: C. GILES

ELECTRO-MAGNETIC APPLICATIONS, INC.
P.O. BOX 8482
ALBUQUERQUE, NM 87108
ATTN: C. MEREWETHER

FAIRCHILD CAMERA AND INSTRUMENT CORP.
464 ELLIS STREET
MAINTAIN VIEW, CA 94040
ATTN: SEC CON FOR D. MYERS

FORD AEROSPACE & COMMUNICATIONS CORP.
FORD & JAMBOREE ROADS
NEWPORT BEACH, CA 92663
ATTN: K. ATTINGER

FORD AEROSPACE & COMMUNICATIONS CORP.
3939 FABIAN WAY
PALO ALTO, CA 94303
ATTN: TECH LIBRARY
ATTN: J. MATTINGLEY

FRANKLIN INSTITUTE
20TH STREET AND PARKWAY
PHILADELPHIA, PA 19103
ATTN: R. THOMPSON

GENERAL DYNAMICS CORP.
ELECTRONICS DIVISION
P.O. BOX 81127
SAN DIEGO, CA 92138
ATTN: RESEARCH LIBRARY

GENERAL DYNAMICS CORP.
INTER-DIVISION RESEARCH LIBRARY
KEARNY MESA
P.O. BOX 80986
SAN DIEGO, CA 92138
ATTN: RESEARCH LIBRARY

GENERAL ELECTRIC CO
SPACE DIVISION
VALLEY FORGE SPACE CENTER
P.O. BOX 8555
PHILADELPHIA, PA 19101
ATTN: J. ANDREWS

GENERAL DYNAMICS
P.O. BOX 748
FORT WORTH, TX 76101
ATTN: P. CURRIER

GENERAL ELECTRIC CO
AEROSPACE ELECTRONICS SYSTEMS
FRENCH ROAD
UTICA, NY 13503
ATTN: C. HEWISON

GENERAL ELECTRIC CO.
P.O. BOX 5000
BINGHAMTON, NY 13902
ATTN: TECH LIBRARY

GENERAL ELECTRIC CO. TEMPO
816 STATE STREET (P.O. DRAWER QQ)
SANTA BARBARA, CA 93102
ATTN: W. MCNAMARA
ATTN: DASIAC
ATTN: R. RUTHERFORD

GENERAL ELECTRIC CO. TEMPO
HUNTINGTON BUILDING, SUITE 300
2560 HUNTINGTON AVENUE
ALEXANDRIA, VA 22303
ATTN: DASIAC

GENERAL RESEARCH CORP.
SANTA BARBARA DIVISION
P.O. BOX 6770
SANTA BARBARA, CA 93111
ATTN: TECH INFORMATION OFFICE (3)

GEORGIA INSTITUTE OF TECHNOLOGY
GEORGIA TECH RESEARCH INSTITUTE
ATLANTA, GA 30332
ATTN: R. CURRY

GEORGIA INSTITUTE OF TECHNOLOGY
OFFICE OF CONTRACT ADMINISTRATION
ATLANTA, GA 30332
ATTN: RES & SEC COORD FOR H. DENNY

GRUMMAN AEROSPACE CORP.
5 OYSTER BAY ROAD
BETHPAGE, NY 11714
ATTN: L-01 35
ATTN: A. CASERTA

GTE SYLVANIA, INC.
ELECTRONICS SYSTEMS GRP - EASTERN DIV.
77 A STREET
NEEDHAM, MA 02194
ATTN: O. THORNHILL
ATTN: L. BLAISDELL

GTE SYLVANIA, INC
189 B STREET
NEEDHAM HEIGHTS, MA 02194
ATTN: C. RAMSBOTTOM
ATTN: E. MOTCHOK
ATTN: M. NUREFORA
ATTN: J. WALDRON
ATTN: D. FLOOD

HARRIS CORP
HARRIS SEMICONDUCTOR DIVISION
P.O. BOX 883
MELBOURNE, FL 32901
ATTN: A. STRAIN
ATTN: V PRES & MGR PRGMS DIV

HAZELTINE CORP.
PULASKI ROAD
GREENLAWN, NY 11740
ATTN: M. WAITE

HONEYWELL, INC.
AVIONICS DIVISION
2600 RIDGEWAY PARKWAY
MINNEAPOLIS, MN 55413
ATTN: S&RC LIBRARY
ATTN: R. JOHNSON
ATTN: G. ANDERSON

HONEYWELL, INC.
AVIONICS DIVISION
P.O. BOX 11563
ST. PETERSBURG, FL 33733
ATTN: W. STEWART
ATTN: S. GRAFF

HUGHES AIRCRAFT CO.
CENTINELA AND TEALE
CULVER CITY, CA 90230
ATTN: J. SINGLETARY
ATTN: CTDC 6/8110
ATTN: K. WALKER

IIT RESEARCH INSTITUTE
10 W 35TH STREET
CHICAGO, IL 60616
ATTN: I. MINDEL
ATTN: J. BRIDGES

INSTITUTE FOR DEFENSE ANALYSES
400 ARMY-NAVY DRIVE
ARLINGTON, VA 22202
ATTN: TECH INFO SERVICES

INTERNATIONAL TEL & TELEGRAPH CORP.
500 WASHINGTON AVENUE
NUTLEY, NJ 07110
ATTN: TECH LIBRARY
ATTN: A. RICHARDSON

ION PHYSICS CORP.
S. BEDFORD STREET
BURLINGTON, MA 01803
ATTN: R. EVANS

IRT CORP.
P.O. BOX 81087
SAN DIEGO, CA 92138
ATTN: D. SWIFT

JAYCOR
P.O. BOX 2008
SANTA BARBARA, CA 93120
ATTN: W. RADASKY
ATTN: D. HIGGINS

JAYCOR
1401 CAMINO DEL MAR
DEL MAR, CA 92014
ATTN: R. STAHL
ATTN: E. WENAAS
ATTN: W. HARDWICK

JAYCOR
205 S WHITING STREET, SUITE 500
ALEXANDRIA, VA 22304
ATTN: LIBRARY

JOHNS HOPKINS UNIVERSITY
APPLIED PHYSICS LAB
JOHNS HOPKINS ROAD
LAUREL, MD 20810
ATTN: P. PARTRIDGE

KAMAN SCIENCES CORP.
P.O. BOX 7463
COLORADO SPRINGS, CO 80933
ATTN: W. STARK
ATTN: J. LUBELL
ATTN: F. SHELTON
ATTN: W. WARE
ATTN: A. BRIDGES
ATTN: W. RICH

LAWRENCE LIVERMORE LABORATORY
P.O. BOX 808
LIVERMORE, CA 94550
ATTN: DOC CON FOR TECH INFO DEPT. LIBRARY
ATTN: DOC CON FOR L96 T. DONICH
ATTN: DOC CON FOR L-156 H. CABAYAN
ATTN: DOC CON FOR L-10 H. KRUGER

LITTON SYSTEMS, INC.
DATA SYSTEMS DIVISION
8000 WOODLEY AVENUE
VAN NUYS, CA 91409
ATTN: M848-61
ATTN: EMC GP

LITTON SYSTEMS, INC.
GUIDANCE & CONTROL SYSTEMS DIVISION
5500 CANOGA AVENUE
WOODLAND HILLS, CA 91364
ATTN: J. MOYER

LITTON SYSTEMS, INC.
AMECOM DIVISION
5115 CALVERT ROAD
COLLEGE PARK, MD 20740
ATTN: J. SKAGGS

LOCKHEED MISSILES & SPACE CO., INC.
P.O. BOX 504
SUNNYVALE, CA 94086
ATTN: E. SMITH
ATTN: B. KIMURA
ATTN: H. THAYN
ATTN: L. ROSSI
ATTN: S. TAIMUTY
ATTN: G. HEATH

LOCKHEED MISSILES AND SPACE CO., INC.
3251 HANOVER STREET
PALO ALTO, CA 94304
ATTN: TECH INFO CENTER

LOS ALAMOS SCIENTIFIC LABORATORY
P.O. BOX 1663
LOS ALAMOS, NM 87545
ATTN: DOC CON FOR C. BENTON
ATTN: DOC CON FOR B. NOEL

LUTECH, INC.
P.O. BOX 1263
BERKELEY, CA 94701
ATTN: F. TESCHE

MASSACHUSETTS INSTITUTE OF TECHNOLOGY
LINCOLN LAB
P.O. BOX 73
LEXINGTON, MA 02173
ATTN: L. LOUGHLIN

MARTIN MARIETTA CORP.
P.O. BOX 5837
ORLANDO, FL 32855
ATTN: M. GRIFFITH

MCDONNELL DOUGLAS CORP.
P.O. BOX 516
ST. LOUIS, MO 63166
ATTN: T. ENDER
ATTN: G. WEINSTOCK

MCDONNELL DOUGLAS CORP.
5301 BOLSA AVENUE
HUNTINGTON BEACH, CA 92647
ATTN: TECH LIBRARY SERVICES
ATTN: S. SCHNEIDER

MISSION RESEARCH CORP.
P.O. DRAWER 719
SANTA BARBARA, CA 93102
ATTN: W. HART
ATTN: ENP GROUP

MISSION RESEARCH CORP.
FM SYSTEM APPLICATIONS DIVISION
1400 SAN MATEO BLVD, SE, SUITE A
ALBUQUERQUE, NM 87108
ATTN: L. MCCORMICK
ATTN: A. CHODCROW

MITRE CORP.
P.O. BOX 208
BEDFORD, MA 01730
ATTN: M. FITZGERALD
ATTN: C. HUSBANDS

NORDEN SYSTEMS, INC.
NORDEN PLACE
NORWALK, CT 06856
ATTN: TECH LIBRARY

NORTHROP CORP.
ELECTRONIC DIVISION
2301 W 120TH STREET
HAWTHORNE, CA 90250
ATTN: LEW. SMITH
ATTN: RAD EFFECTS GRP
ATTN: V. DEMARTINO

OPTELCOM INC.
15940 SHADY GROVE RD.
GAITHERSBURG, MD 70760
ATTN: W. CULVER

PALISADES INST FOR RSCH SERVICES, INC.
201 WARICK STREET
NEW YORK, NY 10014
ATTN: RECORDS SUPERVISOR

PHYSICS INTERNATIONAL CO.
2700 MERCED STREET
SAN LEANDRO, CA 94577
ATTN: DOCUMENT CONTROL

R & D ASSOCIATES
P.O. BOX 9695
MARINA DEL RAY, CA 90291
ATTN: R. SCHAEFER
ATTN: C. MO
ATTN: DOCUMENT CONTROL
ATTN: C. MACDONALD
ATTN: E. GAGE

R & D ASSOCIATES
1401 WILSON BLVD
SUITE 500
ARLINGTON, VA 22209
ATTN: J. BOMBARDT

RAND CORP.
1700 MAIN STREET
SANTA MONICA, CA 90406
ATTN: LIB-D

RAYTHEON CO.
HARTWELL ROAD
BEDFORD, MA 01730
ATTN: G. JOSHI

RAYTHEON CO.
528 BOSTON POST ROAD
SUDBURY, MA 01776
ATTN: H. FLESCHER

RCA CORP.
GOVERNMENT SYSTEMS DIVISION
ASTRO ELECTRONICS
P.O. BOX 800, LOCUST CORNER
EAST WINDSOR TOWNSHIP
PRINCETON, NJ 08540
ATTN: G. BRUCKER

RCA CORP.
DAVID SARNOFF RESEARCH CENTER
P.O. BOX 432
PRINCETON, NJ 08540
ATTN: L. MINICH

RCA CORP.
CAMDEN COMPLEX
FRONT & COOPER STREETS
CAMDEN' NJ 08012
ATTN: C. WHITEHEAD
ATTN: R. ROSTROM

ROCKWELL INTERNATIONAL CORP.
P.O. BOX 3105
ANAHEIM, CA 92803
ATTN: J. MONROE
ATTN: N. RUDIE
ATTN: V. MICHEL
ATTN: C/243-068, 031-CA31

ROCKWELL INTERNATIONAL CORP.
SPACE DIVISION
12214 SOUTH LAKEWOOD BOULEVARD
DOWNEY, CA 90241
ATTN: B. WHITE

ROCKWELL INTERNATIONAL CORP.
815 LAPHAM STREET
EL SEGUNDO, CA 90245
ATTN: B-1 DIV TIC (BADE)

ROCKWELL INTERNATIONAL CORP.
P.O. BOX 369
CLEARFIELD, UT 84015
ATTN: F. SHAW

SANDERS ASSOCIATES, INC.
95 CANAL STREET
NASHUA, NH 03060
ATTN: R. DESPATHY

SANDIA LABORATORIES
P.O. BOX 5800
ALBUQUERQUE, NM 87115
ATTN: DOC CON FOR E. HARTMAN
ATTN: DOC CON FOR R. PARKER

SCIENCE APPLICATIONS, INC.
P.O. BOX 2351
LA JOLLA, CA 92038
ATTN: R. PARKINSON

SCIENCE APPLICATIONS, INC.
2109 W. CLINTON AVENUE
SUITE 700
HUNTSVILLE, AL 35805
ATTN: N. BYRN

SCIENCE APPLICATIONS, INC.
8400 WESTPARK DRIVE
MCLEAN, VA 22101
ATTN: W. CHADSEY

SIDNEY FRANKEL & ASSOCIATES
1165 SAXON WAY
MENLO PARK, CA 94025
ATTN: S. FRANKEL

SINGER CO.
1150 MCBRIDE AVENUE
LITTLE FALLS, NY 07424
ATTN: TECH INFORMATION CENTER

SPERRY RAND CORP.
SPERRY MICROWAVE ELECTRONICS
P.O. BOX 4648
CLEARWATER, FL 33518
ATTN: M. CORT

SPERRY RAND CORP.
SPERRY DIVISION
MARCUS AVENUE
GREAT NECK, NY 11020
ATTN: TECH LIBRARY

SPERRY RAND CORP.
SPERRY FLIGHT SYSTEMS
P.O. BOX 21111
PHOENIX, AZ 85036
ATTN: D. SCHOW

SPIRE CORP.
P.O. BOX D
BEDFORD, MA 01730
ATTN: R. LITTLE

SRI INTERNATIONAL
333 RAVENSWOOD AVENUE
MENLO PARK, CA 94025
ATTN: A. WHITSON
ATTN: E. VANCE

TELEDYNE BROWN ENGINEERING
CUMMINGS RESEARCH PARK
HUNTSVILLE, AL 35807
ATTN: F. LEONARD

TEXAS INSTRUMENTS, INC.
P.O. BOX 6015
DALLAS, TX 75265
ATTN: TECH LIBRARY
ATTN: D. MANUS

TEXAS TECH UNIVERSITY
P.O. BOX 5404, NORTH COLLEGE STATION
LUBBOCK, TX 79417
ATTN: T. SIMPSON

TRW DEFENSE & SPACE SYS GROUP
ONE SPACE PARK
REDONDO BEACH, CA 90278
ATTN: R. PLEBUCH
ATTN: L. MAGNOLIA

SPECTRONICS
830 E. ARAPAHO RD.
RICHARDSON, TX 75080
ATTN: J. R. BAIRD

TRW SYSTEMS AND ENERGY
P.O. Box 368
CLEARFIELD, UT 84015
ATTN: C. PUBSLEY

UNITED TECHNOLOGIES CORP.
HAMILTON STANDARD DIVISION
BRADLEY INTERNATIONAL AIRPORT
WINDSOR LOCKS, CT 06069
ATTN: CHIEF ELEC DESIGN

WESTINGHOUSE ELECTRIC CORP.
ADVANCED ENERGY SYSTEMS DIV.
P.O. BOX 10864
PITTSBURGH, PA 15236
ATTN: TECH LIBRARY

VOUGHT SYSTEMS DIVISION
LTV AEROSPACE CORP.
P.O. BOX 225907
DALLAS, TX 75265
ATTN: P. CUNNINGHAM

VALTEC CORP.
99 HARTWELL ST.
WEST BOYLSTON, MA 01583
ATTN: W. TROUT